NON-INVASIVE MONITORING OF VITAL SIGNS USING RECLINER CHAIR AND RESPIRATORY PATTERN ANALYSIS

A Thesis presented to
the Faculty of the Graduate School
University of Missouri-Columbia

In Partial Fulfilment
Of the Requirements for the Degree
Master in Science

---

by

AKSHITH ULLAL

Dr. Marjorie Skubic, Thesis Supervisor

MAY 2018

The undersigned, appointed by the dean of the Graduate School, have examined the thesis entitled

NON-INVASIVE MONITORING OF VITAL SIGNS FOR OLDER ADULTS USING RECLINER CHAIRS AND RESPIRATORY PATTERN ANALYSIS

Presented by Akshith Ullal,

A candidate for the degree of
Master of Science in Electrical Engineering,
And hereby certify that, in their opinion, it is worthy of acceptance.

Dr. Marjorie Skubic, PhD

Dr. Laurel Despins, PhD

Dr. Mihail Popescu, PhD

To Mizzou…..

ACKNOWLEDGMENTS

Firstly, I would like to thank Dr. Marjorie Skubic, for giving me the opportunity to work at the Eldertech Lab. Her suggestions and criticisms were valuable while conducting my research. I would also like to thank Dr. Mihail Popescu, Dr. Laurel Despins and Dr. James Keller who were also part of the team at Eledertech lab, for their guidance towards my research.

I would like to express my gratitude to all the members at Eldertech Lab, particularly Bo Yu Su, Moein Enayati and Jasmine Jalali for guiding me. Finally, my thesis would not have been possible without the help of the staff and residents at TigerPlace Assisted Living, Columbia, MO whom I am grateful to.

Contents

List of Figures

List of Tables

ABSTRACT

In-home monitoring has the potential to help track health changes for older adults with chronic health conditions, thereby making early treatment possible when exacerbations arise. A recliner chair is often used by older adults, even for sleeping at night, for those with breathing difficulty, neck and back problems, or other pain. Here, we present a sensor system for recliner chairs that can be used to monitor heart rate and respiration rate. The system uses two accelerometers placed strategically to capture these vital signs noninvasively and without direct contact with the body, while at same time being hidden from view. The system was tested with 45 subjects, with an average age of 78.8 years for both upright and reclined configurations of the chair. We also tested the system on 6 different types of recliner models. An accuracy of 99% for heart rate and 93% for respiratory rate was obtained. An analysis of the error distribution patterns according to age, gender and recliner configurations are considered.

A validation study of a commercially available sensor, Murata SCA11H, which is primarily designed for use on the bed is tested on the chair and the results are presented in this thesis. We have also developed a measure known as the "Breathing Pattern Index" that can be useful in determining the respiratory health of the occupants on the chair. Initial studies of the effectiveness of this index and algorithm are evaluated and the results are presented. This new system and index have the potential to help in identifying very early health changes and improve health outcomes for older adults.

Chapter 1

Introduction

This chapter gives an overview of the motivation, problem statement and the primary goals for developing the chair sensor system and the "Breathing Pattern Index".

1.1 Motivation

Monitoring of essential vital signs has become more important than ever, considering the increased risk of cardiovascular ailments today [1]. Of the 56.4 million death which occurred in 2015, 23.4 million deaths were caused due to cardiovascular diseases. Of these 8.76 million were caused by Ischaemic heart disease, 6.24 million by stroke, 3.19 million by lower respiratory infections, 3.17 million by chronic obstructive pulmonary disease and 1.69 million by lung cancers [32]. According to the Centre for Disease Control and Prevention (CDC) around 200,000 deaths caused due to heart diseases can be prevented in the US alone [33]. The lifestyle associated with today's work environment also has a part to play in this. Since most of us work in desktop office environment that requires continuously sitting for long hours, we often do not get adequate exercise to keep our bodies healthy. Hence many people have now started developing these chronic cardiovascular condition in their early forties and fifties. By the time people reach their sixties, they have a host of diseases which drastically decreases their quality of living. This decrease in standard of living and inactivity leads to a host of other psychological problems like depression and loss of self-esteem.

According to the CDC, depression affects 1-5 % of the general elderly population, but about 13.5 % of the elderly that require home health care and about 11 % of the elderly in hospitals [33]. This abnormally high prevalence of depression among the elderly with health problems is a worrying trend. Older adults are at risk of misdiagnosis and lack of treatment because some of their symptoms can mimic normal age-related issues. Symptoms can also be mistakenly attributed to other illnesses, medications, or life changes. Elderly patients might also be reluctant to talk about their feelings or fail to understand that physical symptoms can be a sign of depression. For elderly people

living independently, isolation can make it difficult to reach out for help. In order to combat this problem a new concept known as “Aging in Place” has been adopted at many assisted living homes across the US. “Aging in Place” is defined by the CDC as “ The ability to live in one’s home and community safely, independently and comfortably, regardless of age, income or ability level”. This concept has been fundamental to the many assisted living centres opened in recent years across the US. The main application of the work in this thesis is for continuous health monitoring at these centres.

In-home sensing has the potential to track health and improve health outcomes by continuously and non-invasively monitoring older adults, catching early indicators of health change, and thereby facilitating proactive action to prevent health decline [2]. Many of these in home systems when working in conjunction, can provide a more complete picture of the patient’s health. For example tracking changes in one’s respiratory patterns could give information about impeding heart problems, or tracking patient’s restlessness, amount of time in bed could give an indication about their mental health and wellbeing. Some of the non-invasive technologies include radar to detect falls, depth sensors to capture gait, and bed sensors to capture sleeping patterns. Our sensor system is designed primarily to complement the bed sensor system in providing continuous heart and respiration data, especially at night when older adults sleep on Recliner chairs.

1.2 Problem Statement

Bed sensors have also been proposed for capturing heart rate and respiration unobtrusively, such as the hydraulic bed sensor described in [4], [5]. This hydraulic bed sensor was designed and validated at the Center for Eldercare and Rehabilitation Technology and has been deployed at TigerPlace Assisted living site, Columbia, MO. The bed sensor consists of 4 transducers placed vertically parallel to each other each with a pressure sensor. The goal is to monitor the occupant’s heart and respiratory rates throughout the night so that long-term health changes can be tracked and their effects studied. Alerts can then be sent to the clinical staff if there are anomalies. However, many older adults find it uncomfortable to sleep on the bed due to breathing problems or pain, and instead sleep on recliner chairs.

One of the most common problem that cause breathing difficulty in older adults while sleeping is Congestive heart Failure (CHF). Around 5.7 million Americans have CHF and it is the leading cause of hospitalization in the United States for adults above the age of 65 years. Every year CHF causes around 300,000 deaths [34]. CHF is caused when the pumping force of the heart drops below normal and hence the heart cannot pump enough oxygen to the lungs and other parts of the body. When the heart cannot pump all the blood out, the blood starts to fill in the ventricles and build up, congesting the heart and also causes the fluid to back up especially in the lungs. Generally there are 2 types of heart failure: Systolic and Diastolic. Systolic failure happens when the heart cannot contract or pump blood efficiently while Diastolic failure happens when the heart contraction is normal, but during the relaxation phase, it becomes stiff or rigid. Diastolic heart failure is more common in older adults. Thus the heart is unable to fill properly which causes back up in the lungs, filling the lung sacs with fluid and hence the patient is unable to breathe properly. This problem is exacerbated while lying down. While standing or seating upright the natural force of gravity aides the flow of blood into the heart. Hence older adults with CHF prefer to sleep in recliners so that their breathing becomes easier.

Studies have also shown that CHF leads to apnea, both central and obstructive [35]. Central apnea is caused when the brain does not send proper signals to the lung muscles for breathing, while obstructive apnea occurs when the airway becomes blocked. The two types of apnea can occur simultaneously but usually for CHF patients it begins with obstructive apnea and gradually the central apnea starts. Other causes for avoiding sleeping on the bed are lower back and general body pain. The most common causes of back pain in older adults are osteoarthritis and spinal stenosis. Osteoarthritis is a degenerative condition that develops gradually over time. The pain is caused by the breakdown of the cartilage between the facet joints in the spine. At first the symptoms may only be intermittent, but can later develop into steadier pain in the lower back, and may eventually cause sciatica in addition to lower back pain. From the surveys conducted, older adults say that the soft cushion of the bed does not support the natural structure of the spine, while the recliner chair cushion being stiffer provides a much more comfortable support. Some elders may also have additional problems such as diabetes, which causes them to wake up and frequently use the bathrooms at night. They say it is easier to do this while

sleeping on a recliner than on the bed. Sometimes, elders accidentally fall asleep on the recliners while watching TV or just reading. In all the above cases, we will not be able to obtain the data from the bed. In order to predict and track health changes continuous data is essential and our chair sensor system can be complemented together with the bed sensor to provide this.

Diseases such as CHF generally tend to show subtle changes in the respiratory patterns in advance of the actual diagnosis and preliminary studies are conducted in this thesis to see if we can track these changes using the "Breathing Pattern Index".

1.3 Contribution of this thesis

As mentioned before in the problem statement, a chair sensor system that does the same job as the bed sensor was required to continuously monitor residents heart and respiration rates. In this thesis a sensor system that can do this job is presented. This mainly involves testing the proof of concept of the sensing mechanism, testing the system in the lab and finally testing the system in a real time environment to monitor its efficacy. The sensor system developed here is specially designed for use on recliner chairs which are mainly used by older adults. The sensor used to measure the signals is an accelerometer. The system is tested on 6 different types of recliner chair models and the goal of the developed sensor system is to give accurate results for a wide variety of recliner models.

The locations where the accelerometers are placed on the recliner chair is important. And we have 2 design constraints. First, the accelerometer placed should not be on any surface that would be in contact with the occupant. In other words it should not be on the seat or the backrest of the recliner chair. This is because our sensor system is mainly designed for older adults who may find it discomforting to sit on the recliner with sensors on the cushion of the chair. This thesis explores the best possible locations to obtain the heart and respiration rates. The performances of the accelerometers placed at these design criteria locations are evaluated and accordingly the locations are selected. In order to validate this system a study is conducted on older subjects and the performance of the system is evaluated. The results are presented here. Statistical analysis of the results is also done. General trends with respect to

the accuracy of the heart and respiration rates according to the age and gender of the study participants are evaluated and explanations for these trends are suggested.

A commercially available sensor, the Murata SCA11H is tested on the recliner chair and the results are presented here. The SCA11H was mainly designed to capture the heart and respiration signals by placing it under the mattress or on the frame of the bed. Since it uses the same concept as our sensing system, i.e detecting the heart signals by sensing the transfer of Ballistocardiogram (BCG) signals to the chair or the bed, the SCA11H was tested on the same locations as the accelerometer from our system. A comparison is made between the two sensors and the results are presented here. The Breathing Pattern Index (BPI) is defined and preliminary studies for it are conducted. The BPI can be used as a general measure of the respiratory health of the patient. It is similar to the Rapid shallow breathing Index (RSBI) developed in [35] with one major advantage, that it can be measured in real time with for every breath. Its application on the data obtained from the chair sensor study is shown. The trends in the change in BPI are analysed over time.

Chapter 2

Related Work and Background

2.1 Sensing Technologies

Many types of sensing technologies have been proposed to capture the vital signs in naturalistic living environments. With the growth in electronics, these sensors are becoming smaller in size and hence can be worn on the body [7]. Technologies that monitor these vital signs can be divided into wearable and non-wearable sensors. Many wearable sensors that monitor vital signs are already available in the commercial market; The most well-known of wearable sensors are activity trackers, such as Fitbit which mostly use 3 axis accelerometer to measure fitness parameters such as number of steps taken, distance walked, calories burned, floors climbed etc. These trackers not only give the numbers but can also output the measure that gives the intensity of the activity. Current research has been investigating how to make these wearable sensors more efficient and smaller in size [8, 9].

There have also been many skin patch sensors developed that monitor health parameters and hemodynamics. Generally skin patch sensors use optical infrared photo sensitive resistors. However these sensors are not able to measure deep arterial flow. Hence in [36] a patch sensor is developed that uses RF frequency resonance to monitor the health of the patient by tracking the limb hemodynamics. RF frequency being a lower frequency than IR is less absorbed by the body. Inadequate blood flow can be an indicator of many underlying diseases such as peripheral artery disease (PAD), atherosclerosis, heart failure, ischemic muscle damage, diabetes, and stroke. In severe cases, insufficient blood flow to organs and limbs may lead to common medical problems including myocardial infarction, tissue ischemia, irreversible tissue damage, and organ or limb failure or loss.

In our case, where the target population is older adults in private homes or senior housing, wearable sensors are not the best option, since they may cause discomfort,

irritation and sometimes even cause health hazards leading to rashes and infections [10]. Sometimes seniors are reluctant to use wearable technologies because they don't trust it or understand it's working. They may also feel that the devices are invading their privacy. Also, wearable devices must be worn consistently. For adults with memory related diseases remembering to put the devices back on if removed can be a challenge. These spots of incomplete data can induce a lot of discrepancies while running algorithms on them to track long term health changes. Wearable sensing devices also need to be re-charged, which can be difficult for older adults. Non-wearable sensing devices solve a number of the above problems, especially for older adults.

2.2 Chair Sensor Studies

There have been a number of chair sensors developed using non-wearable sensing technologies. Some of the functionalities of these include posture detection, user activity classification [31], stress recognition, and attention level detection of the occupants of the chair. One of the most basic approaches of sensing the posture of a person in a seated position is to put a pressure sensor mat on the chair, as used in [11]. Here, a commercially developed pressure sensor mat by Tekscan is used to cover both the seat and backrest of the chair. Depending upon the pattern of signals from the pressure sensor, principal components analysis (PCA) is used to determine one of 14 different sitting positions: (1)
seated upright, (2) leaning forward, (3) leaning left, (4) leaning right, (5) right leg crossed (with knees touching), (6) right leg crossed (with right foot on left knee), (7) left leg crossed (with knees touching), (8) left leg crossed (with left foot on right knee), (9) left foot on seatpan under right thigh, (10) right foot on seatpan under left thigh, (11) leaning left with right leg crossed, (12) leaning right with left leg crossed, (13) leaning back, and (14) slouching. The sensing algorithm first classifies whether the person is sitting in a static position or continuously moving and based on that, it uses different sets of training data. An accuracy of 96% was obtained when the system was tested on the same users as the training data and 76% accuracy was obtained when multiple users were tested.

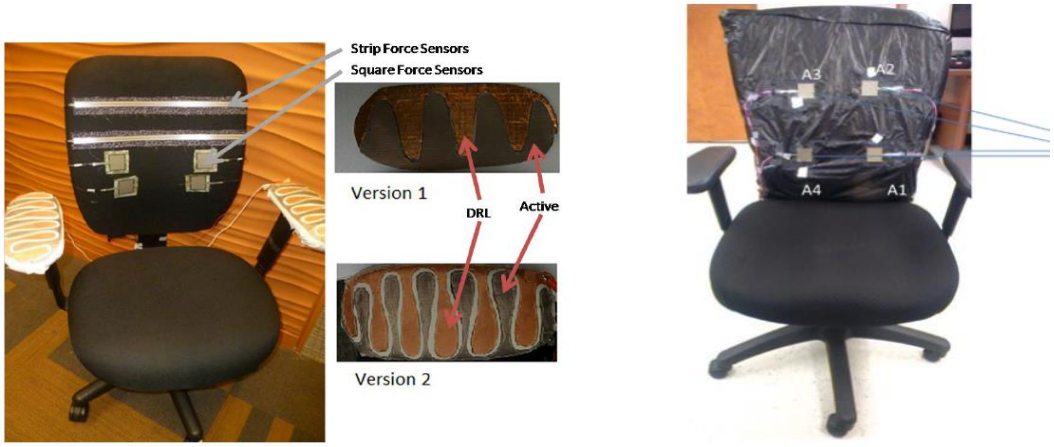

Figure 2.1: Chair sensors used in the related work, that involve placing sensors on the armrest (left) [14] and the backrest of the chair (right) [31].

Figure 2.2: Chair sensors used in the related work, that involve placing an EMFi film on the seat and backrest (left) [14] and a pressure sensor mat (right) [22] .

Using predictive analysis, Fu et al. [12] have developed a chair system that can predict the future activity of the occupant based on his/her current posture. This study uses eight force sensing resistors (FSR) placed at strategic locations, with 4 on the backrest

of the chair to detect back postures (body leaning right, leaning back, body leaning left, no contact) and 4 on the seat of the chair to detect leg postures (sitting upright, crossing right leg on left leg, crossing left leg on right leg, sitting forward, no contact). The future activity is predicted from combining data obtained from the backrest and seat FSRs.

In contrast to the work described in [11], our system is designed primarily for recliner chairs, with the target population being older adults. In [11], the Tekscan pressure sensor mat covers the whole backrest and seat and is primarily designed for chairs with a rigid surface on the seat and back rest. Recliner chairs, on the other hand, are designed with more cushion, and hence the pressure mat may not work as accurately as desired. In addition, the pressure mats and the FSRs in [12] are placed on the surface of the seat and the backrest of the chair, which would make older adults reluctant to use them. Our system uses accelerometers placed at hidden locations (none on the surface of the seat and backrest) and requires little to no modification to the recliner chair.

In [14], a study was conducted on how people sit in chairs and what are their preferences. Based on their preferences, the locations of the sensors were determined. In the study, 50 participants (25 male, 25 female) working mainly in a desk job office environment were interviewed and asked about their sitting position preferences; 67% said they often use the chair backrest, only 6% responded that they never use backrests. Armrests were also used with 38% reporting that they often use armrests and 42% responding that they sometimes use the armrests. Participants were also asked whether they had a primary chair (chair they use for more than 6 hours a day) and 91% responded positively. Of the participants with a primary chair, 94% responded that they had a backrest, and 71% responded that they had armrests. In this study electrocardiogram (ECG) sensors were placed on the armrests, assuming that many occupants may not wear full length sleeves. Although this type of sensing seems may be viable in an office setting, in our case for older adults it becomes a disadvantage. Such skin contact with ECG leads may cause discomfort to older adults due to their more sensitive skin and may also play a part in the spread of rashes and other skin ailments in older adults, which may be a problem due to weak immune systems.

Chair sensors have also been developed to monitor the attention and stress levels of the occupant. Studies have also been done to monitor attention and stress levels of the chair occupants. In [13] Arnrich et al. use the Tekscan pressure mat to calculate the spectra of the norm of the center of pressure (CoP), from which the features are derived to classify the stress levels of the occupants. In the study the participants are required to take part in two activities. One under stressful condition and the other under normal conditions. The subjects were not informed about this and were falsely told that they were participating in a test that correlated cognitive performance with physiological characteristics. The mental stress activity involved solving an adaptive-timed mental arithmetic test under a social evaluation threat (a known person would be continuously monitoring their performance). The controlled condition involved performing the mental arithmetic test with time and social threat limitations. The classification accuracy obtained in this work was around 73.5%. This may be due to not placing sensors in the back and arm rest of the chair.

2.3 Studies Using Ballistocardiogram Sensing

There have been a number of studies conducted using sensors capturing the Ballistocardiogram (BCG) signal, primarily due to its non-invasive nature [15]. BCG signals have been studied for evaluating sleep quality, heart and respiratory patterns [16, 17, and 18] and also identifying cardiac related problems [19, 20, and 21]. There have also been many studies conducted on estimating vital signs, while a person is asleep using BCG signals. In [25] a hydraulic bed sensor is developed that captures the BCG signal unobtrusively when a person is lying on the bed. The sensor system consists of 4 transducers placed vertically under the mattress. Each transducer is a 3 inch wide, 20 inch long flexible tube filled with water, with a pressure sensor placed at one end. The BCG reaction forces are captured by the pressure sensor, caused by the movement of fluid inside of the transducer. Similarly, thin film force sensors can be placed under the bed to obtain the heart rate, when a person is lying in bed as shown in [26]. BCG signals have also been recorded using a static charge sensitive bed (SCSB), although this requires slight modification to the mattress. The BCG signal can also be obtained by placing accelerometers at various locations on the bed.

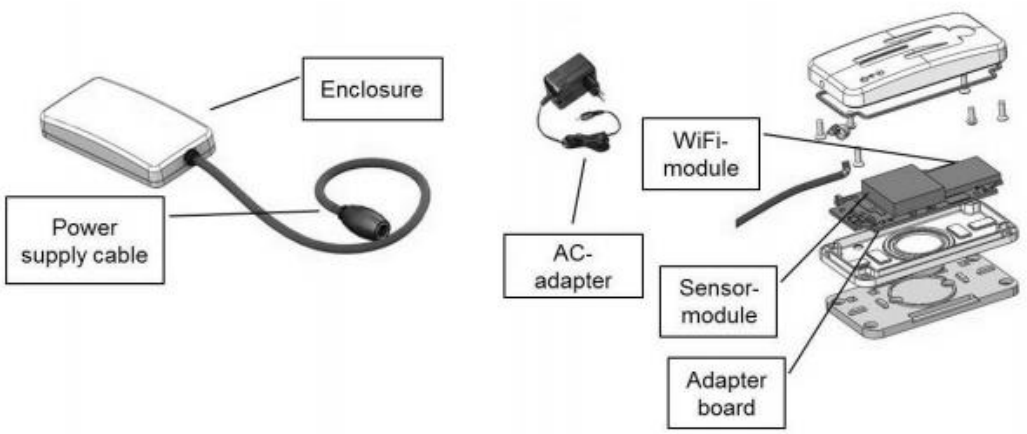

Figure 2.3: The Murata SCA11H sensor system

A commercially available sensor, Murata SCA11H calculates the heart rate from the BCG signal, when placed under the mattress or a metal bed frame. The ability of this sensor to calculate respiration rate accurately can be debatable. A validation study of the SCA11H was conducted in [29]. The main goal of the study was to classify sleep stages, from the heart and respiration rates obtained from the SCA11H sensor. Two SCA11H sensors were placed under the bed, one of them in raw data mode and the other one in processed data mode. In the processed data mode, the SCA11H sensor only outputs the heart and respiration rates, which are calculated using their proprietary algorithms. The reference used in this study for the heart rate was the ECG, and for the respiration a thorax belt. The results showed a correlation between the BCG and ECG of 0.97, but for the respiration rate, the correlation was 0.54.

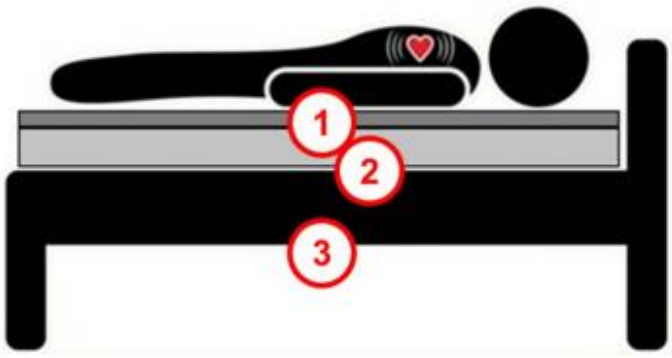

Figure 2.4: Suggested locations for the Murata SCA11H on the bed or bed frame

In [22], the BCG signal is recorded by placing a pressure sensitive EMFi film on the seat and backrest of a chair. The EMFi film is a permanently charged electret film, whose charge distribution changes when pressure is applied. Here, the mechanical pumping action of the heart causes small variations in pressure captured by the film. From these variations, the heart rate is estimated. Although in our study also we use the BCG signal to estimate the heart rate, the design is mainly meant for recliner chairs. The EMFi film design mentioned in [22] is mainly designed for chairs with flat surfaces, which is seldom the case in Recliners. Most of the recliners have curved surface with significant cushion, which may decrease the accuracy of the EMFi film method. Moreover, having a film on their recliners would not be agreeable to many older adults. Our system is designed with all these sensitivities in mind, especially for older adults in the private home and senior living settings.

2.4 Studies Relating to Respiratory Patterns

Generally heart and respiration rates are considered vital signs and monitoring them are of the utmost importance. There are many parameters that are used to gauge a person's respiratory health and different indices can be made from these parameters that can be used to predict the respiratory health outcome of the patient. Below are the definitions of some of these parameters that are used in the related work.

Total Lung Capacity: The volume of air contained in the lungs at the end of maximal inspiration. Generally about 6 litres for an adult male.

Vital Capacity: Maximum amount of air a person can expel after maximum inspiration. The vital capacity of a normal adult varies around 3 to 5 litres.

Residual Volume: The volume of air still remaining in the lungs after the most possible expiration. Generally about 1 – 2 litres.

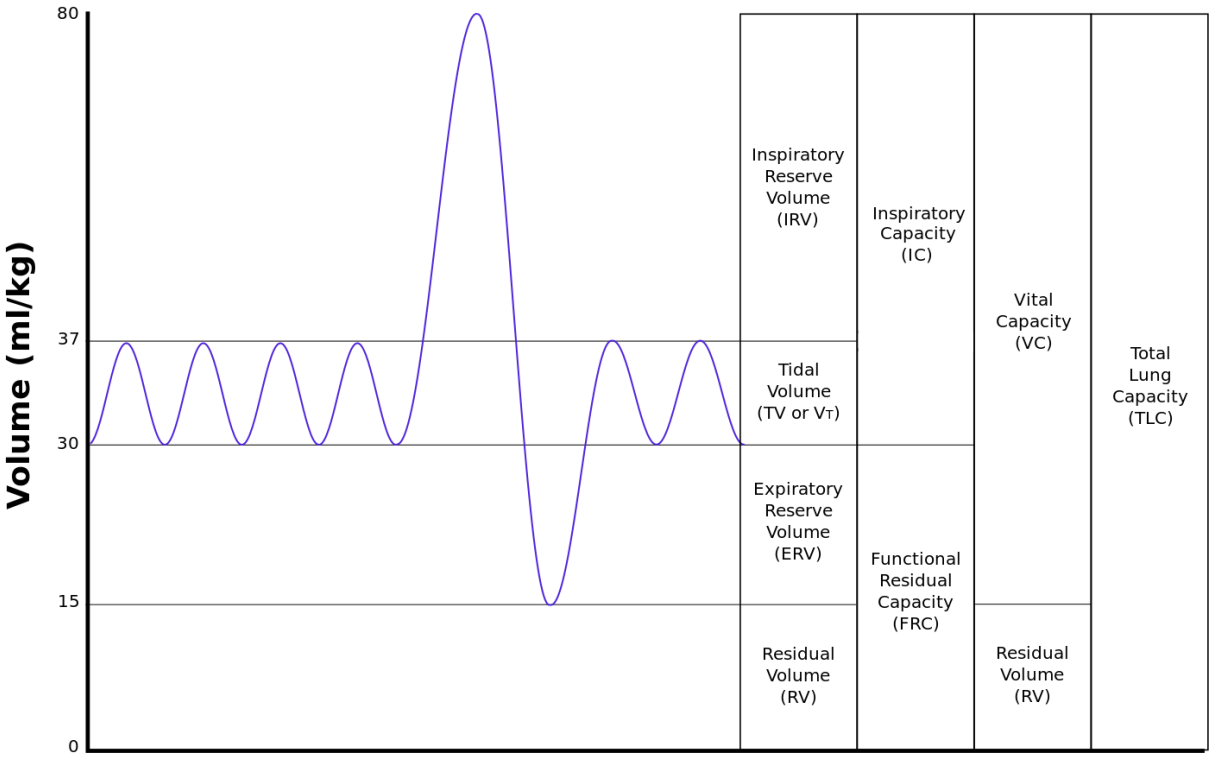

Figure 2.5: Commonly used parameters to measure respiratory health

Tidal Volume: It is the lung volume that represents the normal volume of air displaced between normal inhalation and exhalation when no extra effort is applied. It is generally around 0.5 litres for a normal adult.

Inspiratory Reserve Volume: The maximum amount of additional air that can be drawn into the lungs by a determined effort after normal inspiration.

Previously, some of the above parameters were used to measure a person's respiratory health. For example tidal volume was generally used to measure how healthy one's lungs were and its changes were tracked over time. However the problem with monitoring only these parameters is that their predictive capacity varies from patient to patient. Also they don't take into account some of the pathophysiological factors of breathing. Hence there are new indices being developed that consider some of the above factors.

One such indices that was developed was the Rapid Shallow Breathing Index (RSBI) first shown in [35]. It is defined as the ratio of the respiratory frequency to the tidal volume. In [35], RSBI is used in predicting the outcome of trials of weaning from a mechanical ventilator. Generally only very experienced physicians may be able to tell the outcome of whether weaning a patient from a ventilator will be a success. Hence there needs to be a predictive index that less experienced health care professionals can use to successfully wean a patient from a mechanical ventilator. The motivation for developing the RSBI was to find the earliest time a patient can be weaned and resume spontaneous breathing and also predict if weaning the patient would likely fail, so that cardiorespiratory distress or collapse can be avoided.

Another index was also developed in [35] known as the CROP (Compliance, Rate, Oxygenation, and Pressure) index. The exact definition is given in [35]. It takes into account the pulmonary gas exchange in the lungs while predicting the outcome of weaning. The application of these 2 indices was tested on 100 patients with the mean age of 59.6 years. The RSBI was the most successful predictor of successful weaning having a correlation of 0.97. An RSBI value greater than 105 breaths/min/L was found to be highly predictive of weaning failure while a value below 105 breaths/min/L was found to be able to predict successful weaning of the patient. However the RSBI does not perform as expected when a patient is suffering from neuromuscular diseases [37].

The RSBI is quite popular and it is displayed on most modern ventilators. However it is sensitive to the way the input parameters are measured. A survey among respiratory therapists found that some of them use continuous positive airway pressure (CPAP) while measuring RSBI, while some therapists use pressure support ventilation (PSV) which could affect the readings [38]. In addition to this, it is important to note that diseases such as sepsis and respiratory infections that increase the respiratory frequency effect the RSBI value. The values can also be affected by fever, sleeping in supine position, anxiety, whether ET Tube used, gender and suctioning technique [39-41].

Some therapists have also been sceptical about using RSBI. In a study conducted in [42], 304 patients were randomly divided into 2 groups. For one group, the RSBI was measured, but not used to make a decision to wean the patient, while in the other the

RSBI was the key factor used to decide whether to wean a patient or not. Patients who passed the 2h Spontaneous Breathing Trial (SBT) were eligible for an extubation attempt. The study found that the median duration for weaning time was significantly shorter when the RSBI was not used. There are specific populations where RSBI may not be successfully used for prediction of weaning. A study of using RSBI on patients with Chronic Obstructive Pulmonary disease (COPD) found that the RSBI measured during the SBT was not helpful in predicting successful weaning [43]. It is also no surprise that the RSBI does not work for neuro-surgical patients, since the reason for intubation in these patients in usually airway protection rather than abnormal lung physiology. Hence they will not have problems with their tidal volume or respiratory rate measurements.

Recently, there have also been modifications proposed to the RSBI. Two of the main ones proposed are Serial RSBI and RSBI rate. Usually RSBI is measured at the SBT period. The requirement for measuring it at specific continuous intervals stems from the fact that for some patients the breathing pattern may be stable initially but may deteriorate later. This may be due to poor respiratory muscle endurance especially in older adults. In [45] it is shown that, when RSBI is measured at every 30 minutes the weaning outcome significantly improves.

The “Breathing pattern Index” is similar to the RSBI, but is much easier to measure and track continually. In the RSBI, the measurement of tidal volume cannot be done instantaneously. Our index can give a value for every respiration breath and hence is more sensitive than the RSBI.

Chapter 3

Methodology

This chapter briefly describes the sensor system developed, the device testing methods used and touches upon the signal processing techniques applied to extract the heart and respiration signals from the data. We capture these vital signs by recording the Ballistocardiogram (BCG) signals of the occupant. BCG signals are caused due to the mechanical pumping action of the heart which causes slight expansion and contraction of the arteries and vessels in the circulatory system. These variations are transferred to the chair, which can be captured by a sensitive accelerometer. The detailed sensing mechanism and accelerometer locations are shown in the subsequent subsections.

We are also interested in comparing the performance of the Murata SCA11H on the recliner chair. Although the Murata sensor was designed to be used on the bed or bed frame, the sensing mechanism used by it is the same as our system, i.e. it consists of an accelerometer that measures small variations caused on the bed cushion due to the flow of blood in the body. The testing procedure is given in detail in this section. We also apply the Breathing Pattern Index (BPI) to the data of the subjects who participated in the chair sensor study. It has to be kept in mind that the BPI is calculated as a ratio and hence we are interested only in its relative value to track the changes over time and compare the values between subjects whose signals are captured with devices using the same sensing mechanism.

3.1 BCG Sensing Mechanism

The working of the human heart is analogous to a mechanical pump. When the muscles of the heart contract and expand, they exert forces, which makes blood flow through the vessels in the body. If we imagine the body as an external box, with the heart exerting pressure waves inside of the box, from Newton's third law, there is an opposite reaction from the box to the force exerted on it by the heart and blood flow. That is exactly what a ballistocardiogram (BCG) signal is. A typical BCG signal is shown in Figure 3.5. It is the

reaction of the body to the pumping forces of the heart. When an occupant is sitting on the chair, these reaction motions are transferred (with losses) to the chair, which we capture using an accelerometer. We are generally interested in capturing the J-peak of the BCG signals, since it has the largest amplitude and hence most easily captured. The consortium of h, i, j, k, l, m and n peaks consist of 1 heartbeat. In many cases h, m and n peaks may not be seen. The accuracy of the reading from the accelerometer depends on its sensitivity and also its location, when placed on the chair.

3.2 Recliner Chair Basic Design

Although recliner chairs come in different shapes and sizes, their underlying design and structures are similar [24], which makes our sensor system deployable across a wide range of chairs. Generally, the older recliner models tend to be much larger and bulkier in size compared to the present day design. All recliners have a basic frame, over which the cushion is placed. In older chairs, the frame is generally made of wood, while in newer models it is made of lightweight materials like aluminium or metal alloys. On top of this frame, lateral springs are placed on both the backrest and the seat of the recliner chair. Finally, there is the lever mechanism that reclines the chair. In many cases the lever mechanism is a manual one that reclines the chair and also brings out the footrest forward. If the lever mechanism is manual, there is a more space under the recliner, since the mechanical arrangement runs through the side of the chair not blocking access to the under cushion of the recliner. However many older adults prefer the automatic recliners due to their ease of use and less effort required to recline the chair. In this case, the space under the recliner is slightly more constrained, due to the hydraulic pumping mechanism that reclines the chair.

Recliners also come with variety of types of cushion materials. A few assortment of them can be seen in Figure 3.3 on which we have tested our system. The top 3 types of chairs in Figure 3.3 have tighter cushion types. The tighter type of cushion are much more suited to the chair sensor system since they transfer the BCG signal variations without much loses on to the accelerometer much easily. However during our testing all these factors were not specifically selected, but the chairs were selected randomly as we wanted our sensor system to be deployed across a wide variety of recliner model.

Figure 3.1: Accelerometer placed on the side of the seat cushion, hidden between the seat cushion and the arm of the chair

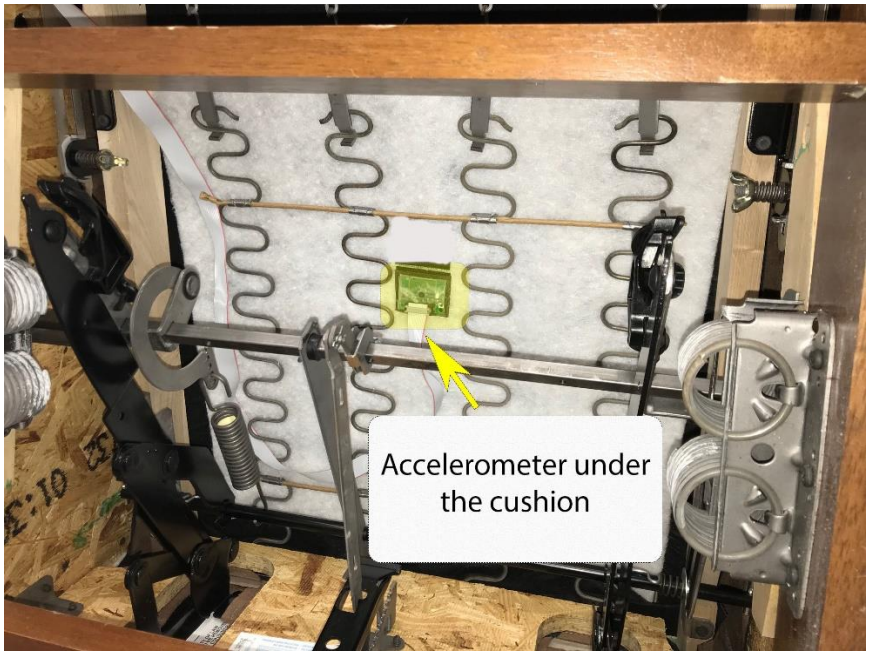

Figure 3.2: Accelerometer placed under the seat cushion of the Recliner chair

3.3 Accelerometer Placement

We had two design considerations while selecting the sensor location, the obvious one being the signal strength captured by the accelerometer, but we also wanted the location of the accelerometer where it would not be visible, not cause discomfort and also require little modification to the recliner chairs so that a retrofit could be easily done. For example, the sensors in previous works were sometimes placed on the backrest or the seat of the chairs. In our case, this would cause serious discomfort to older adults as the sensors will slightly protrude out of the cushion. A case could also be made for embedding a sensor inside the cushion of the recliner chair, but this would require modifications.

Age:	Gender:	Height:	Weight:	Date Time:
Have you ever been diagnosed with any of the following in the past six months?				

Yes	No	Have you drunk Coffee, Tea, or Alcohol in the past 6 hours?
Yes	No	Heart problems (such as heart surgery, heart attack, irregular heartbeat, CHF)?
Yes	No	Lung problems (COPD or emphysema)?
Yes	No	Do you any kind of Sleep apnea diagnosis?
Yes	No	Do you ever have chest or heart pain?
Yes	No	Do you lose your balance because of dizziness / do you ever lose consciousness?
Yes	No	Are you currently taking medication for high blood pressure or heart condition?

Table 3.1: Questionnaire required to be filled by the study subject

Also, if the sensor failed, replacing it would be cumbersome. Many older adults have their recliners customized according to their specific needs and do not prefer them to be changed. Hence the selected locations should not alter the chair in a noticeable manner. After preliminary testing, two locations which fit the design criteria were selected for more extensive tests. As shown in Figure 3.1 and Figure 3.2, these include (1) under the seat cushion, and (2) on the side of the seat cushion, hidden between the seat cushion

and the arm of the chair. The accelerometers are attached to the recliner chair cushions using Velcro®tapes.

Figure 3.3: 6 different types of recliner chair models tested in the study. The top 3 represent chairs that are bigger in size and that have a harder cushion.

3.4 Sensor System

The system contains 2 Kionix KXR94-2283 accelerometers, shown in Figure 3.4, which have a sensitivity of 1000 mV/g and cost around US $5 each. The accelerometer used to calculate the heartrate is placed under the cushion, slightly forward of the gluteus muscles of the occupant. The accelerometer is secured using a Velcro tape and requires a 5V dc voltage to function. In some recliners this cushion, will be exposed, and can be reached easily by just tilting the chair. In others it may be covered, or there may be

space constraints due to the hydraulic system (in automatic recliners). When the bottom of the recliner chair is covered, a small incision can be made through the cover so that the accelerometer can be taken through it. In either case, with slight modifications, the accelerometer can be placed in the right location. The other accelerometer is placed on the side cushion parallel to the gluteus muscles of the occupant as shown in Figure 3.2.

Figure 3.4: The Kionix KXR94 - 2283 accelerometer development board. Note the accelerometer is the centre black IC

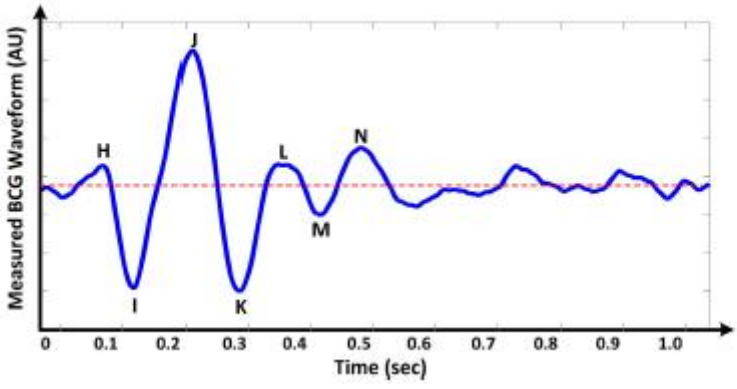

Figure 3.5: A typical BCG signal consisting of the h, i, j, k, l, m and n peaks.

The accelerometers output readings in 3 axes (x, y and z), although accurate heart and respiration signals can be obtained from the z-axis alone. The Kionix accelerometer can output both analog and digital outputs. The following shows the different modes of operation:

Mode 00 – The three outputs (X, Y, Z) are read through the digital SPI interface, which is also used to command Selftest and Standby Mode. The digital I/O pads are powered from a separate power pin, and will interface to 1.8V logic.

Mode 01 – The three outputs (X, Y, Z) are provided on three analog output pins. The KXR94 also features an integrated 3-channel multiplexer (X, Y, Z). The Enable pin must be high for normal operation and low for power shutdown.

Mode 10 – The three outputs (X, Y, Z) are provided on three analog output pins. The KXR94 also features an integrated 4-channel multiplexer (X, Y, Z, Aux In). The Enable pin must be high for normal operation and low for power shutdown.

Mode 11 – The three outputs (X, Y, Z) are provided on three analog output pins. The KXR94 also features an integrated 4-channel multiplexer (X, Y, Z, Aux In). The Enable pin must be low for normal operation and high for power shutdown.

We have used the accelerometer in Mode 10. Although the accelerometer itself can output digital signals, we use the analog output and convert it to a digital signal externally using a data acquisition device (DAQ) for accuracy purposes.

For testing the device with subjects, we used the National Instruments USB 6212 DAQ with a sampling frequency of 100 Hz. The reason for using the DAQ is that it can be directly connected via USB to a computer, and the output can be viewed in real time. Deployment in naturalistic home environments will require an embedded system (a future goal).

3.5 Signal Processing Methods

Once the data pre-processing is complete, we apply our signal processing algorithms to the raw data. We did not apply any hardware based filtering to the Analog signals obtained from the accelerometers, since this may result in loss of information, and most of our subjects are older adults, tending to have weak and noisy signals. We have data

coming in from 4 sensors, i.e. 2 accelerometers, one placed on the under the seat cushion and the other on the side cushion.

.

Figure 3.6: Two chair positions were tested in the study: Upright (left) and Reclined (right). For ground truth reference, a chest band and a finger pulse transducer were worn by each study participant.

We then have data coming from the ground-truth sensors, i.e. the pulse transducer placed on the left index finger, and data from the thorax chest belt. These signals are inputted to the Analog channels of the DAQ. The DAQ samples it at 100 Hz, and we have 10 minutes of data for both the upright and reclined positions of the recliner. The data from the DAQ can be stored in a memory card or even be uploaded on to a server. We then apply software filtering to the signals. The applied filter configurations are both same for the ground truth and the sensor data. We have used Infinite Impulse Response (IIR) – Butterworth filter of the 6^{th} order for the filtering. The Butterworth filter was chosen due its flat (stable) magnitude response in the passband. In order to capture the respiration signal we have used a low pass filter with the cut – off frequency of 0.7 Hz. To capture the heart-rate a band-pass filter with lower cut – off frequency of 0.7 Hz and higher cut-off frequency of 10 Hz was used. We will be using the Hilbert transform method described in [5], for calculating the heartrate, and using the peak detection algorithm for calculating the respiration rate.

3.5.1 Heart Rate Calculation

The Hilbert transform method was used in [5], primarily for pulse rate estimation from Ballistocardiogram (BCG) signals obtained from a hydraulic bed transducer. Since our accelerometers are also capturing BCG signals, we also use the same algorithm, with slight modification in our transducer (accelerometer) signal modelling. In the HT method we try to most accurately estimate the heart rate by analysing the signal in the frequency domain. The main idea is to divide the signal into smaller segments using a Hamming window, and apply the Hilbert transform method for each of them. We apply this method for the signals obtained from the accelerometer placed under the cushion, used to calculate the heartrate. The signal obtained from the under cushion accelerometer can be represented as:

$$a_1(t) = r(t) + p(t)\cos(2\pi f_0 t) + \varepsilon(t) \quad (1)$$

Here $r(t)$ represents the respiration. We can see a typical BCG signal as shown in Figure 3.5. It can be observed that the J peak has the largest amplitude, and we are interested in detecting this peak, as it is the most pronounced. Hence the number of J peaks detected per minute will be our heart-rate estimate. The J peaks are modelled by the *p(t)*, which is a periodic pulse digital signal, with the same frequency as the heart-rate. The h, i, k, l and m peaks are represented by the $\cos(2\pi f0t)$ with the modulation frequency f_0 of around 4 Hz, since there are h, I , k, l, and m peaks. Most of the times m or h peaks are not seen and hence we have chosen a round figure of 4 Hz for f_0. The *ε(t)* signal here represents the noise. This includes both low frequency noise caused due to movements and also high frequency additive noise introduced from the environment and electronic equipment. This can be removed by passing the signal through a band pass filter. We then apply a low pass filter to remove with cut-off frequency of 0.7Hz, to remove the low frequencies of *ε(t)* .

$$a_1'(t) = BPF\left(a_1(t)\right) = p(t)\cos(2\pi f_0 t) + \varepsilon'(t) \quad (2)$$

$$g(t) = a_1'(t) + j a_1(t) \quad (3)$$

We then apply the Hilbert transform to the filtered signal, which will cause a 90 degree phase shift as shown in equation (3). A 90 degree phase shift will result in $j a_1(t) = p(t)\sin(2\pi f_0 t)$ which is an accurate approximation when the noise signal is low and

can be ignored. This works in the HT algorithm method because we compute the confidence level for each segment window and reject that segment if the confidence is low, In other words, we do not evaluate window segments of the signal which are noisy, and hence the above approximation is fairly accurate.

We then take the magnitude of *g(t)*, which will result in isolating the *p(t)* signal required for the heart rate estimation.

$$k\,(t) = \,|g\,(t)\,|^2 \;\approx p\,(t)^2 \qquad (4)$$

k(t) represents the square of the pulse train, and applying Fast Fourier transform (FFT) to $p\,(t)^2$ will give its frequency spectrum. The highest amplitude frequency is selected, and this will be the heart-rate estimate. Since the sensor signals obtained are non-stationary, we will need to apply windowing method, for stationary signal analysis techniques like FFT to be valid. All of the above shown steps of the HT method is applied to a segmentation window of 60 seconds, with it sliding 15 seconds every iteration. This results in a 75% overlap with every consecutive window.

The above method of calculating heart rate, may give accurate results only when the signal to noise ratio is good, since this is an assumption in (4). Hence we need a gauge to calculate the SNR in each window segment. This is done by computing the confidence level for each 60 second window segment. The exact algorithm is shown in [5], but the mathematical notation for computing the confidence is shown below:

$$conf = \frac{|G\,(\widehat{\theta})|}{(\int_{0.7}^{10}|G(f)|/df)/9.3} \qquad (4)$$

It is a simple ratio of the selected frequency power to the average of the rest of the spectrum frequency. The integration range here is the cut off frequencies of the band pass filter used with the lower cut off frequency of 0.7 Hz and higher cut off frequency of 10 Hz. The factor k is to take into account false harmonic peaks. The value for k is decided as shown below:

$$k\left(\hat{\theta}\right) = \begin{cases} 1, & \hat{\theta} < 90 \\ 0.54 + 0.46\cos\left(\frac{(\hat{\theta}-90)\pi}{150}\right), & 90 \leq \hat{\theta} < 240 \\ 0, & otherwise \end{cases} \quad (5)$$

From experimental studies, a confidence of 25k is selected as the threshold. If the confidence value is below 25k, then the segment is rejected.

3.5.2 Respiration Rate Calculation

To get the respiration signal from (1), we need to separate the high frequency components, which is done using a low pass filter with 0.7 Hz as the cut-off frequency, as described above. We then detect the peaks in the resulting low frequency signal. The average respiration rate is calculated by counting the total number of peaks (which is detected where the derivative of the signal is a minimum in a window segment) in the total signal of the subject and dividing it by the time interval to get the breaths/minute. The same calculation is done on both the accelerometer and the chest band (ground truth) signals. Then their error percentage is calculated relative to the ground truth.

Age (years)	**Male**	**Female**	**Total**
55 - 60	2	4	6
61 - 70	1	6	7
71 - 80	4	4	8
81 - 90	3	12	15
91 - 100	4	5	9
Total	14	31	45

Table 3.2: Study participant's age and gender distribution

3.6 Sensor Testing

As noted earlier, the main goal of our sensor system is to monitor older adult's vital signs when they sleep on their recliners. Hence we tested its performance based on both

the upright and reclined positions of the chairs. All of the participants in the study were above 55 years of age with the average age of the 45 subjects being 78.8 years. The testing of the sensor system was done at the TigerPlace Aging in Place senior housing site [28] in Columbia, Missouri. The study was approved by the University of Missouri Institutional Review Board (IRB).

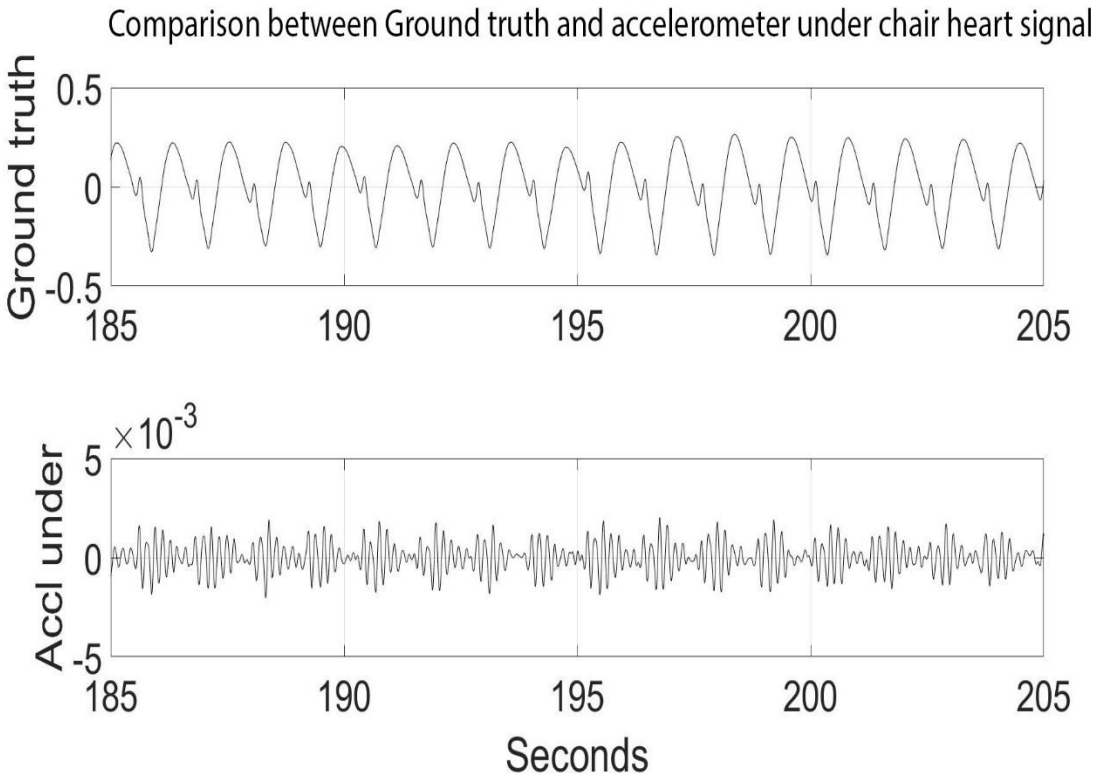

Figure 3.7: The pulse signal obtained from the finger transducer (top) and the BCG signal obtained from the accelerometer (bottom) placed under the recliner seat cushion (Subject ID: 1234).

Each subject wore a finger sensor and a chest band for ground truth reference signals. For calculating the heart rate ground truth, the AD Instruments TN1012/ST pulse transducer was used, (a piezo-electric sensor), which was placed on the left index finger of each subject. For the respiration signal ground truth, the AD Instruments MLT1132 piezo respiratory belt transducer was used. This belt is worn around the chest of the occupant. The data collection included 10 minutes with the chair in the upright position and another 10 minutes with the chair in the reclined position. The angle of recline was considered as the maximum the chair could extend. The reclined position also included

extending the foot rest to the maximum angle, as shown in Figure 3.6. Hence the subject will be in an almost supine position. The subjects were told to relax, and also encouraged to take a nap. Although the subjects were encouraged to remain stationary, their explicit movements were not restricted, as these abnormal movements that cause higher acceleration values will be characterized as restlessness.

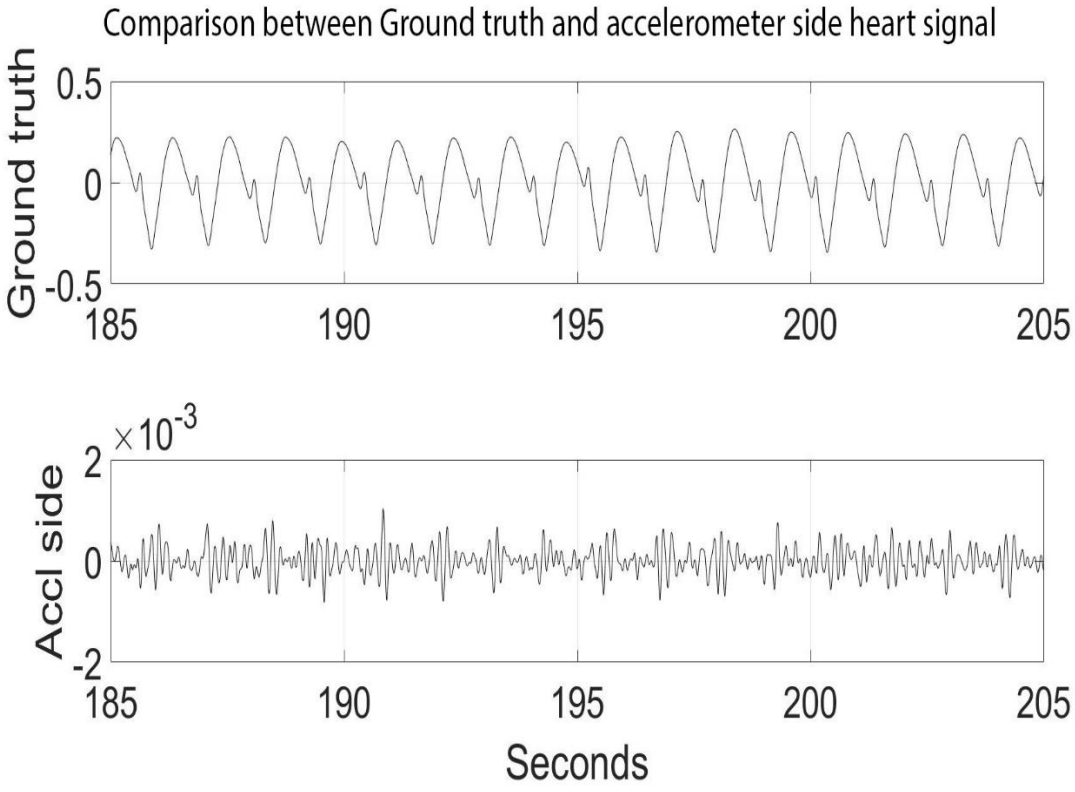

Figure 3.8: The pulse signal obtained from the finger transducer (top) and the BCG signal obtained from the accelerometer (bottom) placed side of the recliner seat cushion (Subject ID: 1234).

There were 45 subjects in total who participated in the study; their age and gender distribution is shown in Table 3.2. Other information recorded included their body measurements of height, weight, age and gender as well as their health as shown by the questionnaire in Table 3.1. Subjects were asked if they had heart problems, such as recent heart attacks, surgeries, congestive heart failure (CHF) and arrhythmia. They were also asked about sleep apnea, and lung problems which included chronic

obstructive pulmonary diseases (COPD) such as emphysema. A note was also made of the medications taken by each subject. There were 13 healthy subjects and 32 non-healthy subjects (having at least one of the above mentioned ailments).

3.7 Respiration rate interval calculation

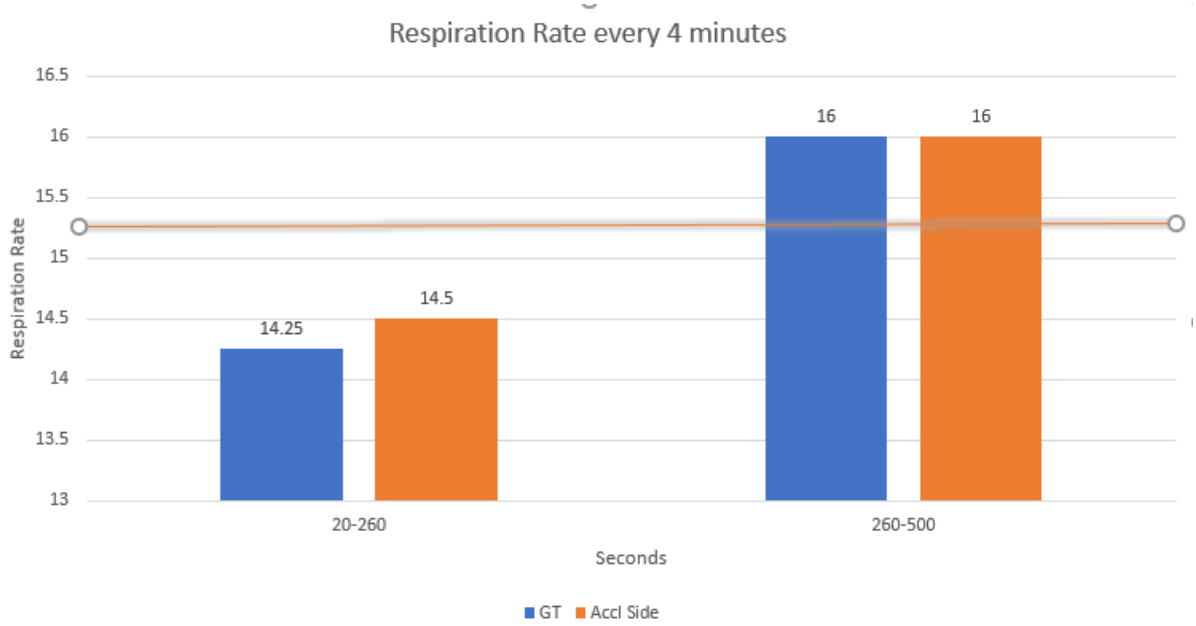

Figure 3.9: Respiratory rate variation calculated every 4 minutes (Subject ID: 1233)

While calculating the respiration rate, we calculated the average respiration rate for the entire 10 minutes. This was done by detecting the peaks for the entire 10-minute signal and dividing it by the time interval. We know that the respiration rate is not constant along the 10 minute interval, especially for unhealthy subjects with lung problems. Hence we wanted an interval to calculate the respiration rate that shows these variations and at the same time not be very computationally intensive. We had a sample size of only 2 subjects with lung problems. Shown below is the respiratory rate variation for a subject with ID: 1233. This subject had been diagnosed with asthma. In Figure 3.9 the respiration rate was calculated every 4 minutes and we see a stark difference between the first and last 4 minutes of the interval. The first and the last minute of the 10 minute interval was not taken into account due to the occupants adjusting or making themselves comfortable on the recliner chair, which introduces noise. When we took the average every minute we could see more clearly the variations. On taking the average every 15 seconds with a 1 minute window a similar pattern was observed. A similar trend was obtained with the other subject with lung problem.

Hence we have decided to report the respiration rate every minute in the future deployment of the system.

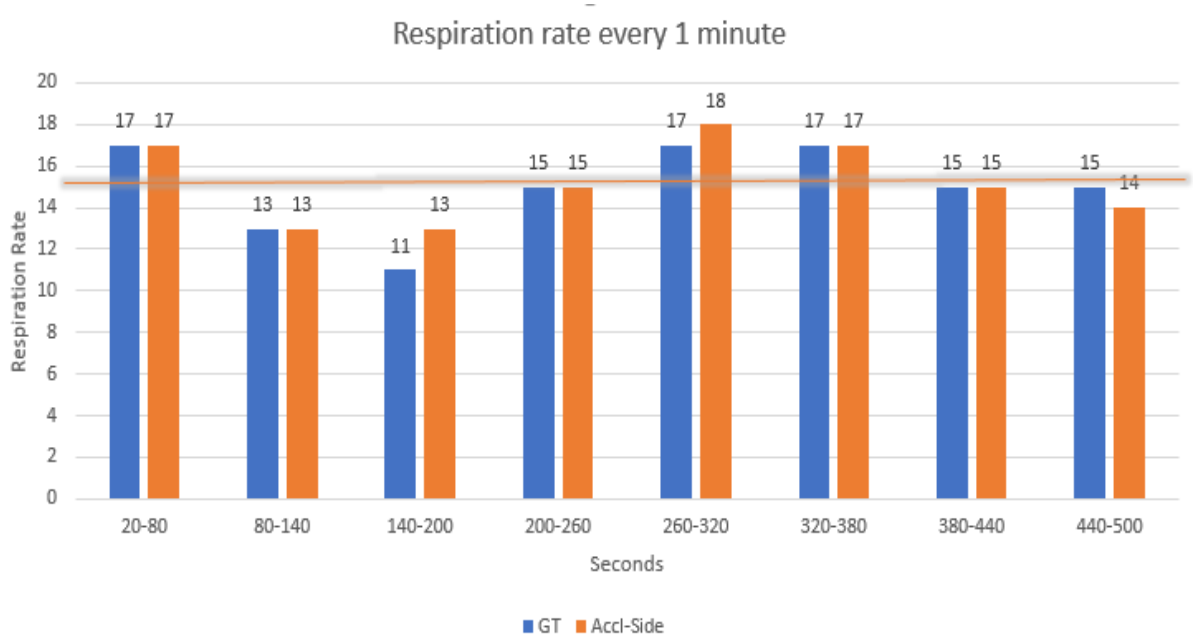

Figure 3.10: Respiratory rate variation calculated every 1 minute (Subject ID: 1233)

Figure 3.11: Respiratory rate variation calculated every 15 seconds (Subject ID: 1233)

3.8 Murata SCA11H Sensor Testing

The MURATA SCA11H is a commercial bed sensor developed by a Japanese company Murata Electronics. It is an embedded system device, which comprises of an accelerometer to collect the raw data, a microcontroller to process the raw data and a Wi-Fi module to transmit the collected data. The commercially available version is enclosed in a water and dust proof casing, which has been rated till IP55. Unlike our Kionix accelerometer, which gives separate acceleration values in 3 different directions(x, y and z axis), the Murata sensor gives the acceleration values only in one dimension.

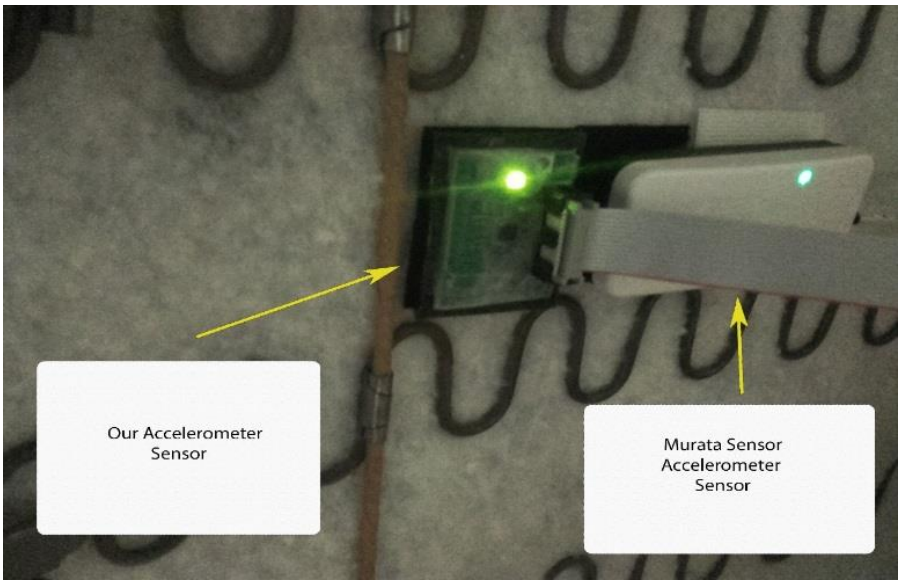

Figure 3.12: Location of the Murata sensor under the chair

The SCA11H can be used to connect to a local server or to the server in the cloud. It transmits the data using Wi-Fi. Once connected to the network the data collection can begin. It is very important to position the Murata sensor appropriately, i.e. it has to be in the same direction of the head to toe as shown on the depicted human figure on top of the accelerometer. Since we have already selected the accelerometer locations, the Murata sensor was placed side by side to our accelerometer to compare the data received from both the devices. The Murata sensor outputs data in 2 modes i.e. the

processed and the raw data mode. They operate mutually exclusively, i.e. it cannot give data in both modes at the same time.

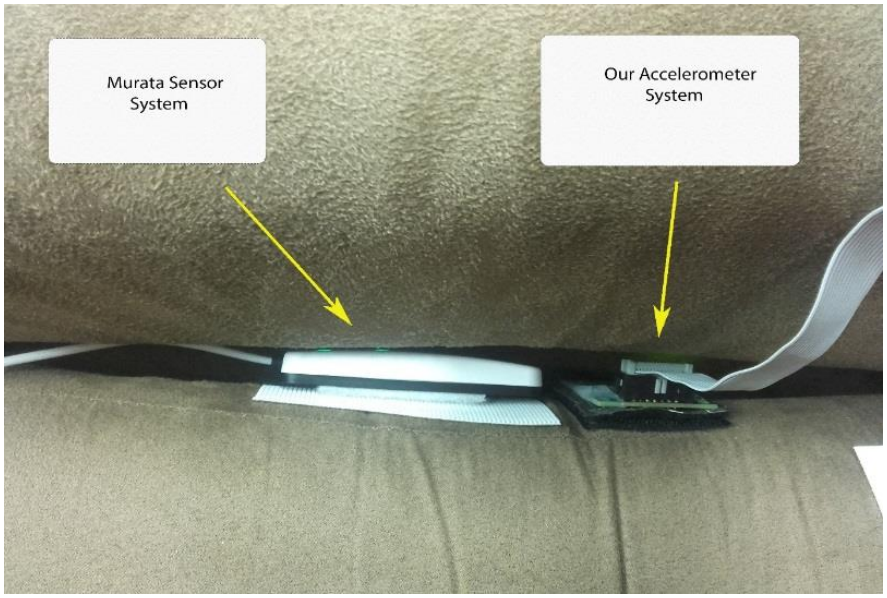

Figure 3.13: Location of the Murata sensor on the side cushion

Calibration: The Murata sensor requires to be calibrated to the bed or the chair. It is a twostep process and has to be conducted in a disturbance free environment. First, it has to be done when no occupant is on the chair. This process takes around 1 minute. Then the occupant is required to sit on the chair or bed, but he has to be stationary and this process also takes about a minute. It is recommended that the calibration is done every time a new person sits on the chair to obtain accurate results.

Modes of operation: The Murata sensor has 2 modes of operation, the processed mode and the raw data mode. In the processed data mode the sensor itself will calculate the parameters through their proprietary algorithms and output these parameters. The outputted parameters are Time stamp, Heart rate, Respiration rate, Stroke volume, Heart rate variability, and the status of the signal. These parameters are outputted every second. All of the outputted data is in the ASCII format. In the raw data mode the data from the accelerometer inside the SCA11H is transmitted. The sampling frequency used

is 1 kHz. The data format used is hexadecimal. Both of the modes of the Murata sensor are tested and the obtained data is shown in the Chapter 5.

3.9 Calculating Breathing Pattern Index on Chair Sensor Subjects

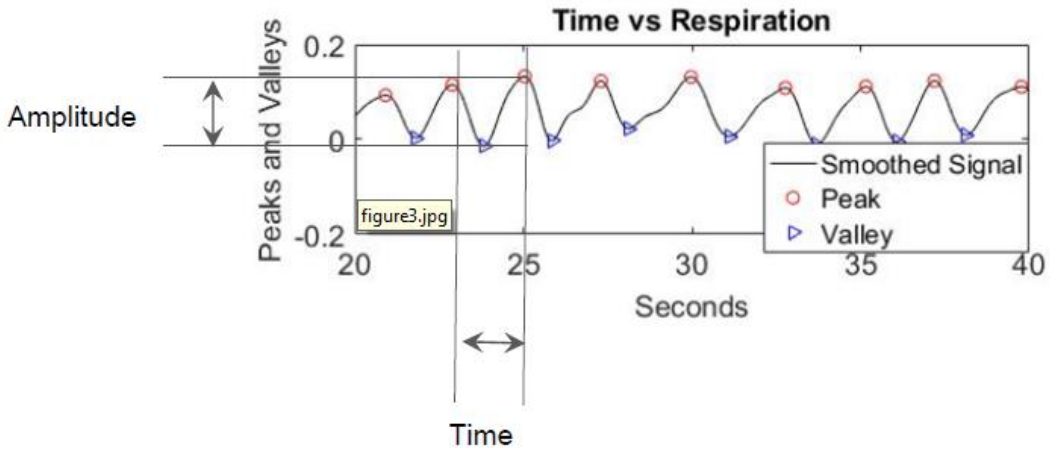

Figure 3.14: Calculation of the Breathing Pattern Index

In [35], the Rapid Shallow Breathing Index (RSBI) was introduced as a measure to predict successful weaning of a patient from the ventilator. It was defined as the ratio of the respiration frequency to the measure of the tidal volume. Tidal volume is defined as the difference between the inspired and expired volume of air during normal breathing. The problem is that the measurement of the tidal volume is a cumbersome process and generally involves the spirometer. Hence we are not able to get the instantaneous value of the RSBI. To calculate the RSBI a person has to blow into the spirometer or have an endotracheal tube inserted into the airway, which is a very invasive process. We have improved upon this, by changing the denominator to the amplitude of the signal, i.e. the difference between the consecutive peak and trough of the respiration signal.

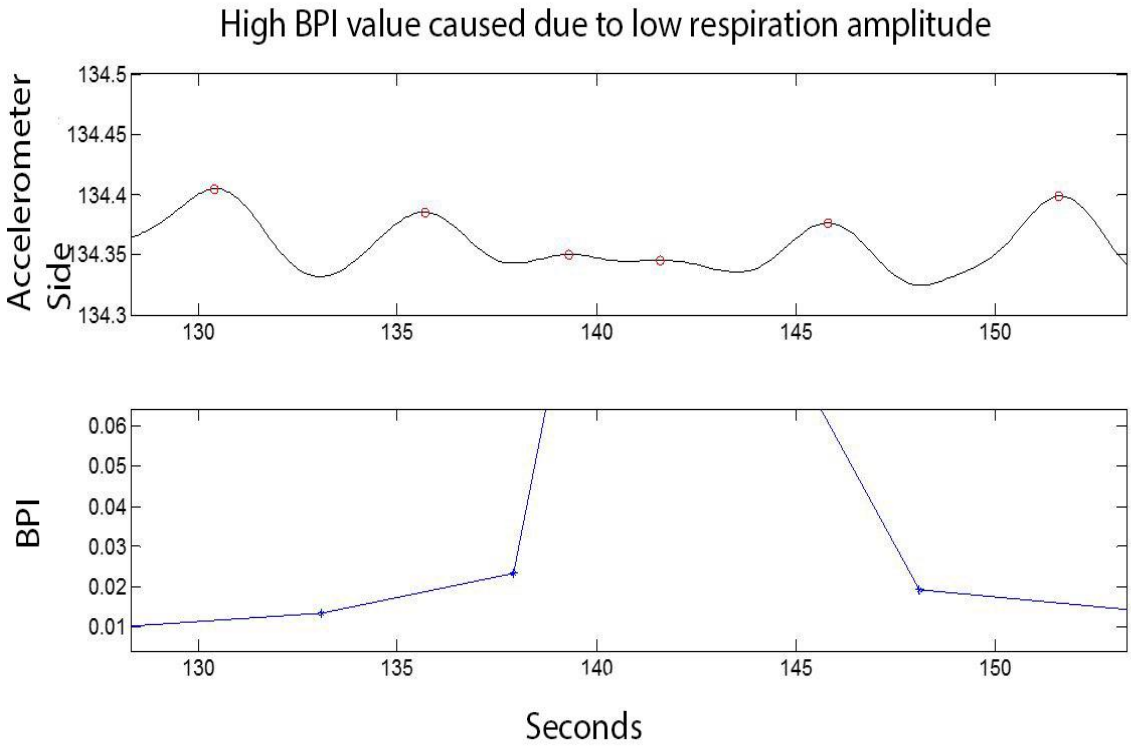

Figure 3.15: High BPI due to low amplitude.

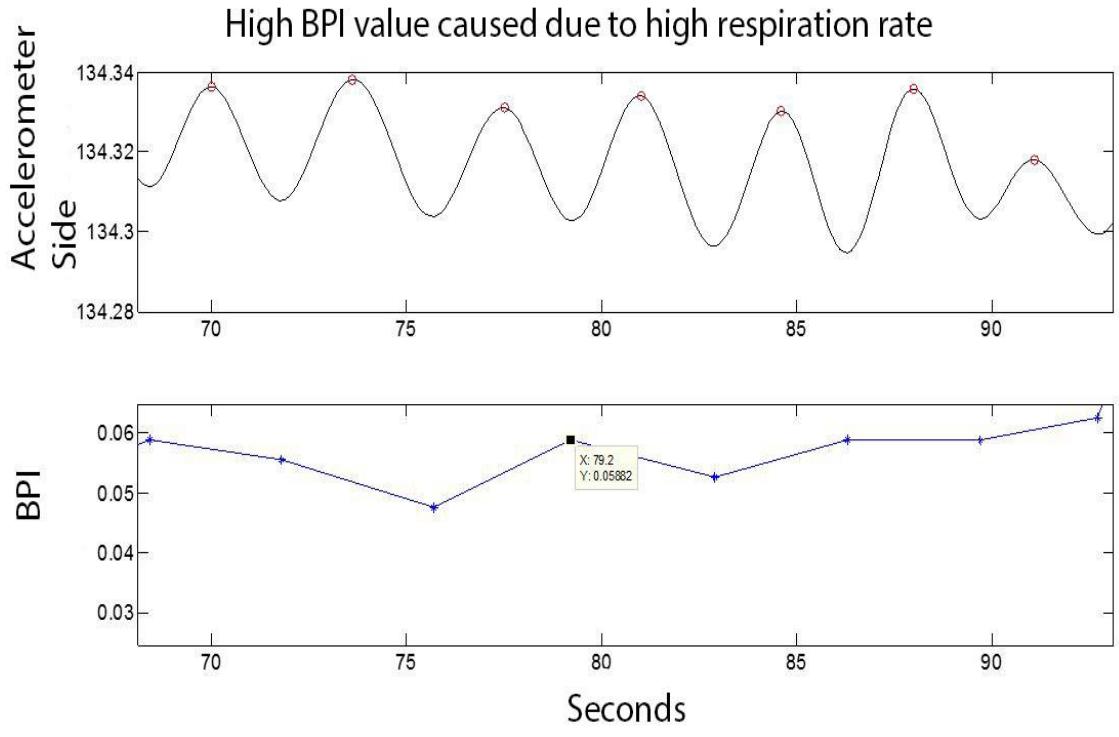

Figure 3.16: High BPI due to high respiration rate.

The definition of the Breathing Pattern Index [46] is shown below:

$$Breathing\ Pattern\ Index\ (BPI) = \frac{Respiration\ rate}{Amplitude\ of\ consecutive\ crest\ and\ trough} \quad (6)$$

The BPI is designed to be a relative index, in the sense its values or units depend on the sensing mechanism used, since the denominator in (6) may be of different units. We are really interested to use the index to track health changes over time and to see if it is able to predict the occurrence of a health problem well in advance of the actual symptoms appearing. Only preliminary studies for the chair sensor subjects regarding the BPI are presented in this thesis and currently we are investigating more on this topic. The behaviour of the BPI is similar to that of the RSBI and hence it will be easy for clinicians to grasp it. Generally unhealthy respiratory signals correspond to higher BPI and healthy signals to lower values of BPI. This is due to the fact that short and fast breaths are usually associated with a person having difficulty in breathing. As shown in Figure 3.15 the BPI goes high when the amplitudes between the corresponding peak and through gets small. The BPI (shown in Figure 3.16) is also high when the respiration rate increases. The signals shown in Figure 3.15 and Figure 3.16 are from the same subject. When compared relatively the difference in BPI values can be seen clearly.

Chapter 4

Results

In this section, the results of the chair sensor system are analysed. Particular emphasis is given on which accelerometer location gives good quality signals and a comparison is made with the ground truth. The results of the Murata sensor are also analysed in comparison with our accelerometer system.

4.1 Heart Rate Results

4.1.1 HT Algorithm Average Percentage error

The formula for calculating this error is shown below:

$$Error\ (\%) = \frac{1}{N}\sum_{i=1}^{N}\frac{\left|GT(i)_{avg} - Est(i)_{avg}\right|}{GT(i)_{avg}} \times 100 \quad (7)$$

$$GT(i)_{avg} = \frac{1}{M}\sum_{k=1}^{M} GT(k) \quad (8)$$

$$Est(i)_{avg} = \frac{1}{M}\sum_{k=1}^{M} Est(k) \quad (9)$$

where $GT(k)$ is the ground truth heart rate for each window, $Est(k)$ is the HT algorithm estimate for each window, M is the total number of windows for each subject and N is the total number of subjects in the study. If a low confidence for a particular segment is obtained, the corresponding segment for the ground truth signal is also ignored while calculating the error. An example is shown in Table 4.1. Left of the table is the HT Algorithm estimate obtained for the accelerometer. On the right is the same algorithm applied to the pulse transducer data (ground truth). Notice that for 2 segments in the accelerometer the estimate is 0. This means that the estimate of the algorithm has a confidence below 25k, which is the threshold used in the HT Algorithm. 0 is just an arbitrary number. Hence when calculating the HT algorithm average estimate for this

subject, only 80.612 and 77.774 are considered for the accelerometer and the corresponding values of 80.556 and 77.454 are considered for the ground truth.

HT Algorithm estimate (Accelerometer)				**HT Algorithm estimate (Ground truth)**			
80.612	0	0	77.774	80.556	79.742	79.010	77.454

Table 4.1: Example of the HT Algorithm average estimate

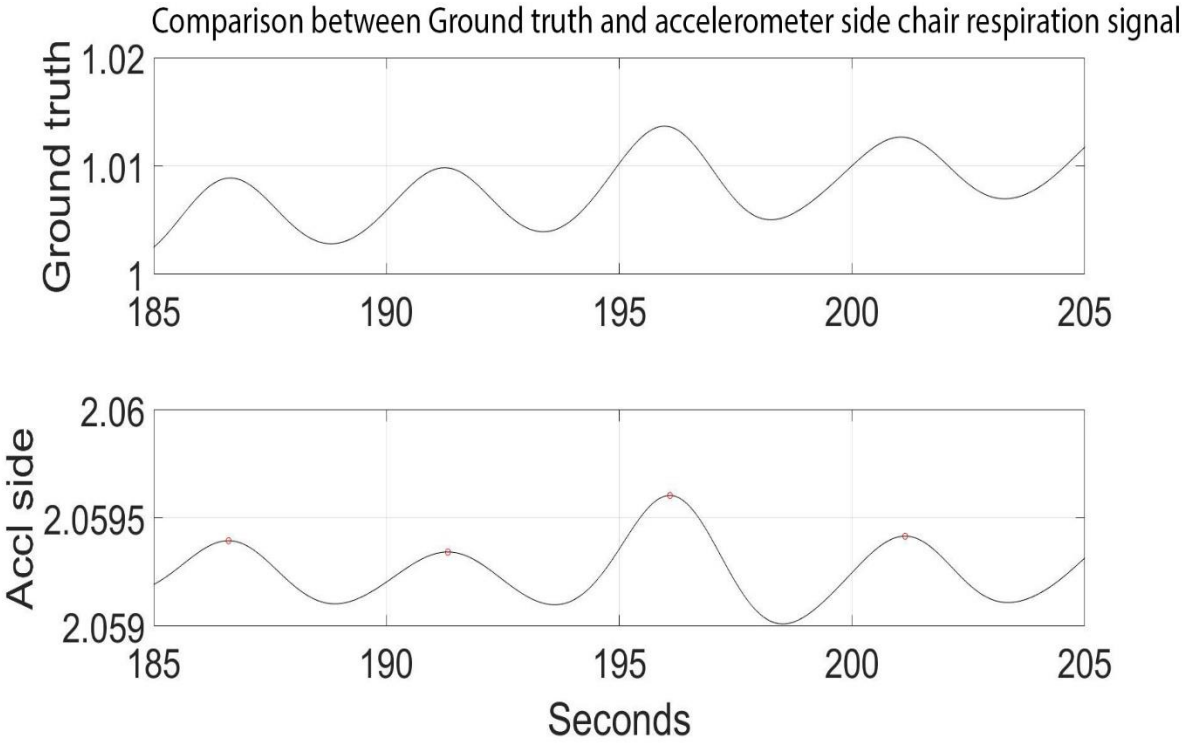

Figure 4.1: The respiration signal obtained from the chest band (top) and the signal obtained from the accelerometer (bottom) placed on the side of the recliner seat cushion.

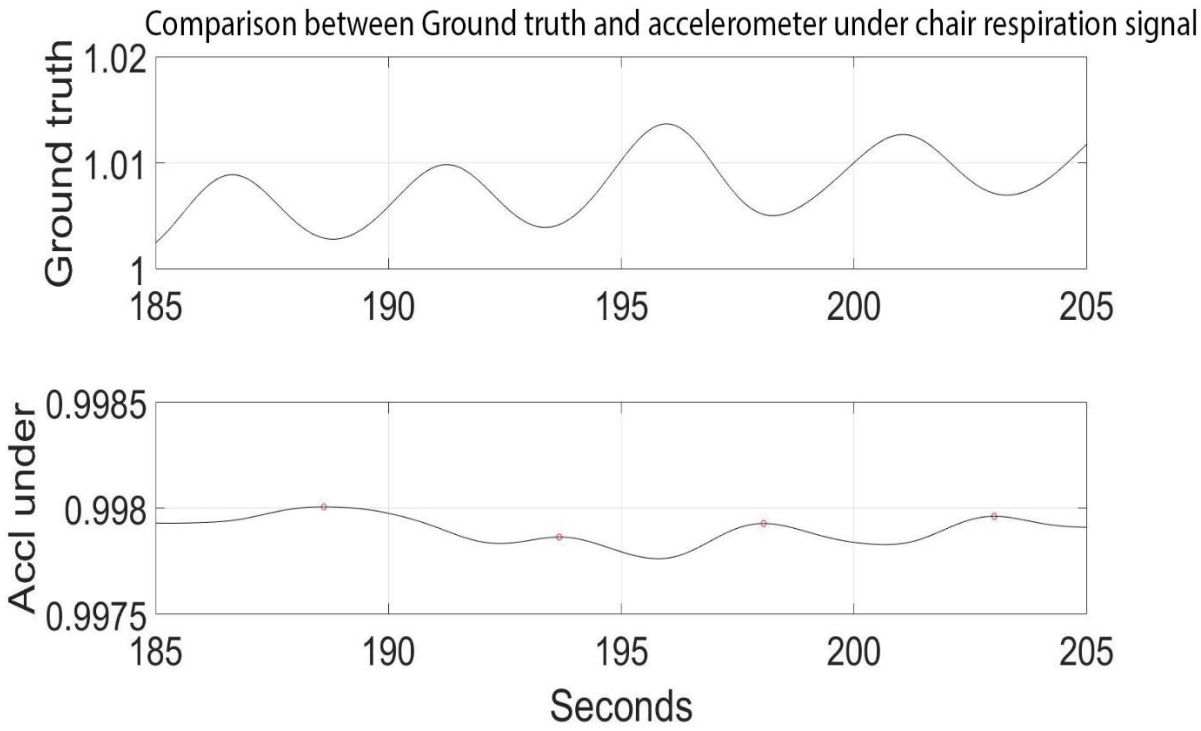

Figure 4.2: The respiration signal obtained from the chest band (top) and the signal obtained from the accelerometer (bottom) placed under the recliner seat cushion.

Figure 3.7 shows the BCG signal obtained from the accelerometer placed under the recliner chair (Subject ID: 1234). The plot on top of the figure shows the signal obtained from the pulse transducer (ground truth) and the bottom plot shows the one from the accelerometer. It can be seen that the BCG signal is quite clean and an accurate estimate can be obtained from the signal. These signals are fed into the HT Algorithm as the input and the output estimate is obtained. In comparison to the accelerometer placed under the cushion, Figure 3.8 shows the results from obtained from the same subject in the same 30 second interval from the side accelerometer. The J peaks in the signal from the under accelerometer are very pronounced. Hence we can see for the heart signal the accelerometer placed under the cushion gives a clearer signal. Although we can slightly see the J peaks in this subject for the side accelerometer, the result becomes nosier as the subjects become older. This trend becomes clear when we plot the Bland Altman plot for all the subjects as explained later in this section.

Figure 4.2 shows the respiration signal obtained from the under accelerometer (bottom) with the signal obtained from the chest band (ground truth) on top. We can see that the signal is not in sync with the ground truth respiration signal. On the other hand the signal from the side of the accelerometer is shown in Figure 4.1. Here the respiration signal is in sync with the ground truth. In fact this is what we find when looking at the signals from all the subjects tested in the study as shown in the Bland Altman plots for the respiration signals in Figures 4.7 to Figure 4.10.

4.2 Bland Altman Plots

A Bland Altman (BA) plot is a graph that is plotted to show the effectiveness of a new method in predicting the outcome relative to the ground truth or gold standard. It can be seen as a graphical technique used to compare 2 methods of measurement. It is most commonly used in the medical statistics field, especially to test the efficacy of a newly devised method in predicting accurate results. It can also be used to compare 2 types of clinical measurements that may produce some form of error. In a BA plot, the x-axis consists of the average quantity of the two types of measurement and the y-axis consists of the difference between them. In our case there are 45 subjects and we compare the accelerometer values with the ground truth. Hence for a particular subject we take the accelerometer and the ground truth value, plot the average of them on the x-axis and their difference on the y-axis. This step is repeated for all the subjects. A logarithmic scale can also be used if the variations are very large.

Plotting of the mean (blue line in Figures 4.3 – 4.10) and standard deviation (dotted red line in Figures 4.3 – 4.10) of the differences on the y-axis allows for identification of different types of biases. The mean difference is the estimated bias and the standard deviations measure the random fluctuations around the mean. If the mean value of the difference differs significantly from 0, this indicates the presence of a fixed bias. If this bias is consistent then the value can be subtracted from the measurements of the new method to make it more accurate. The 95% limits of agreement is shown by the 1.96* standard deviation line plotted on both sides of the mean difference. If these values are not large it means that the two methods can be used interchangeably. However the limits of agreement line cannot be used in all cases and become unreliable when the sample size is small.

The BA plots for the different configurations of the chair are shown below. There are 4 plots for the heart rate and 4 plots for the respiration, each having the results plotted for both the under and the side accelerometer, both in the upright and reclined positions.

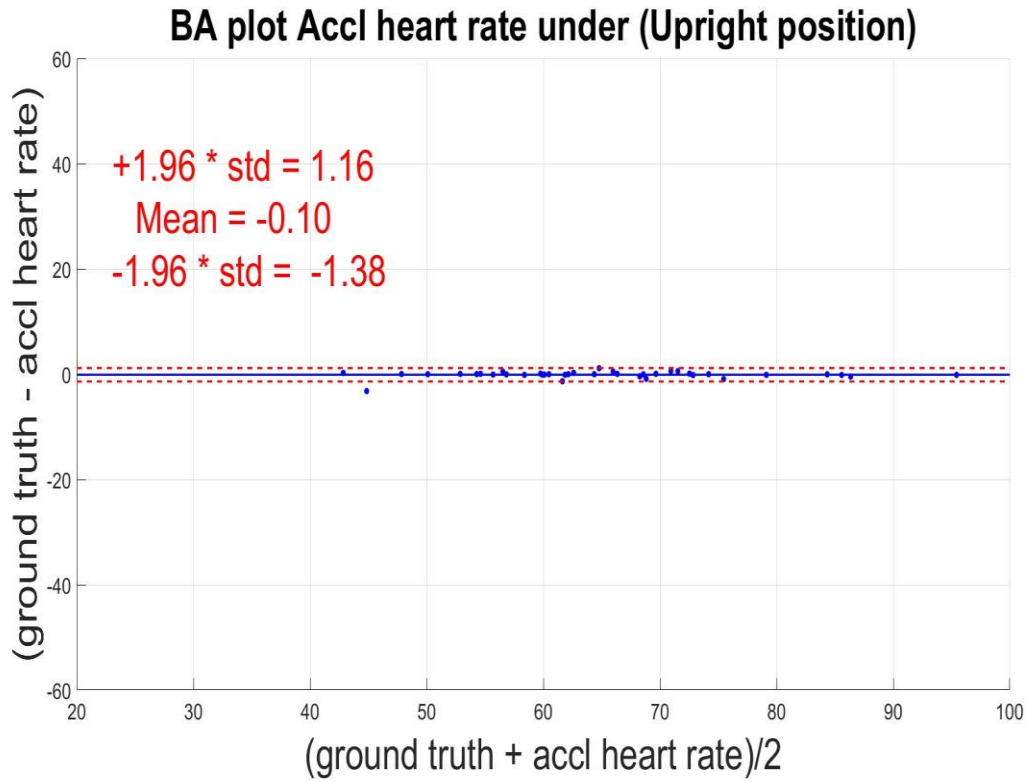

Figure 4.3: Bland Altman plot for the accelerometer placed under the seat cushion and ground truth average heart rate in the upright position.

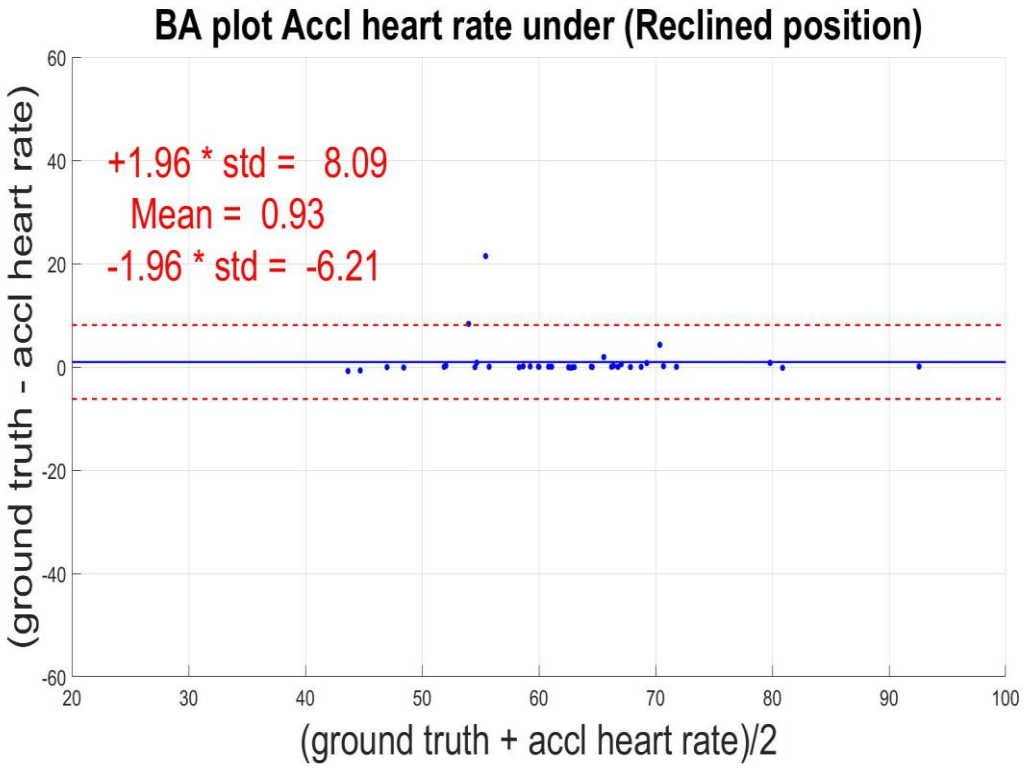

Figure 4.4: Bland Altman plot for the accelerometer placed under the seat cushion and ground truth average heart rate in the reclined position.

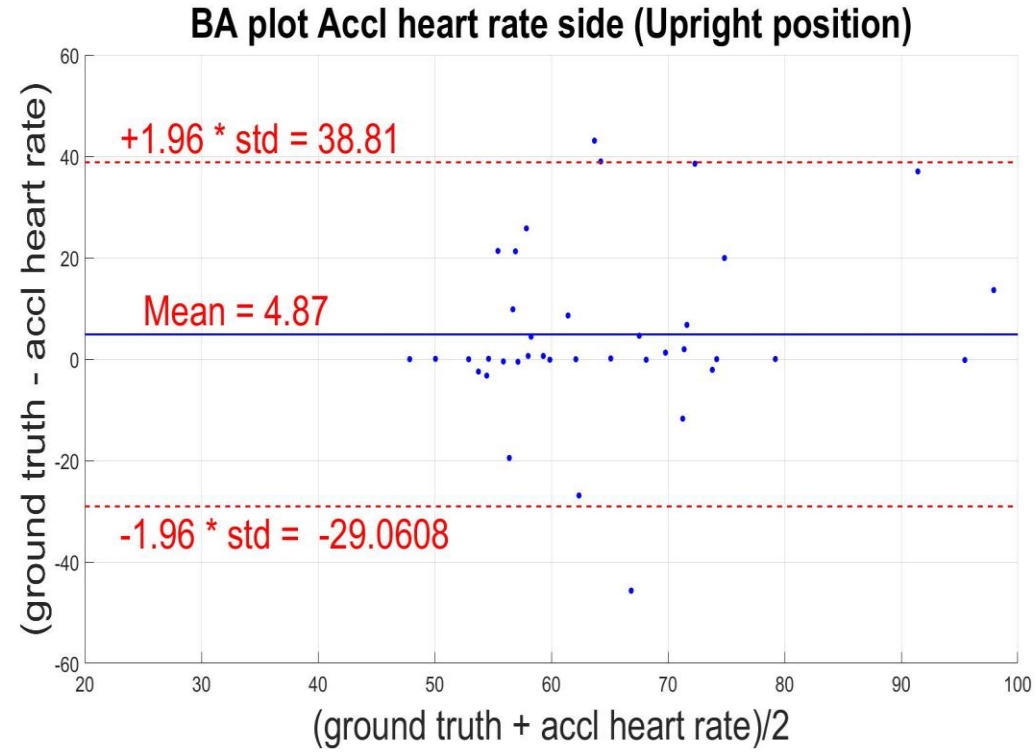

Figure 4.5: Bland Altman plot for the accelerometer placed on the side of the seat cushion and ground truth average heart rate in the upright position.

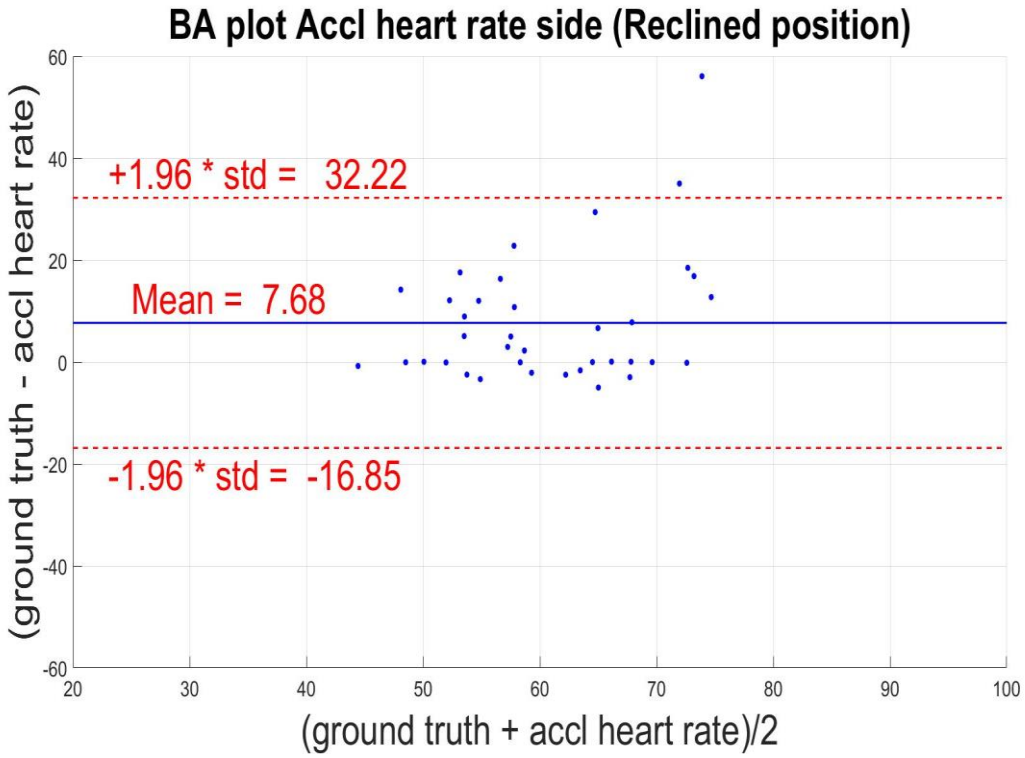

Figure 4.6: Bland Altman plot for the accelerometer placed on the side of the seat cushion and ground truth average heart rate in the reclined position.

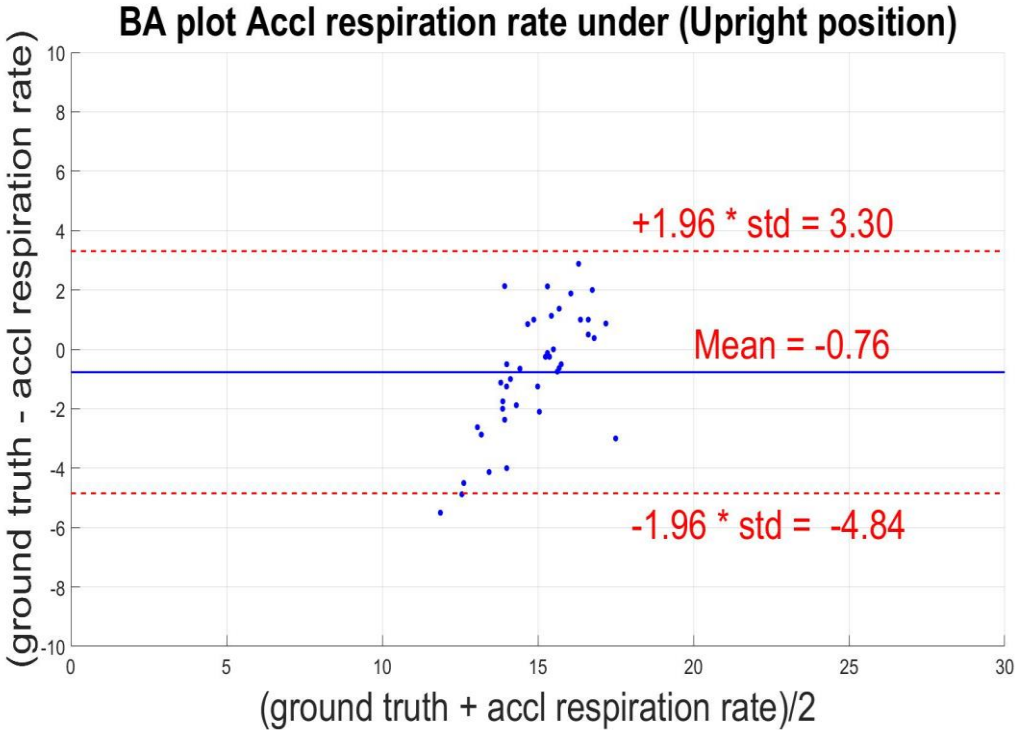

Figure 4.7: Bland Altman plot for the accelerometer placed under cushion and ground truth average respiratory rate in the upright position.

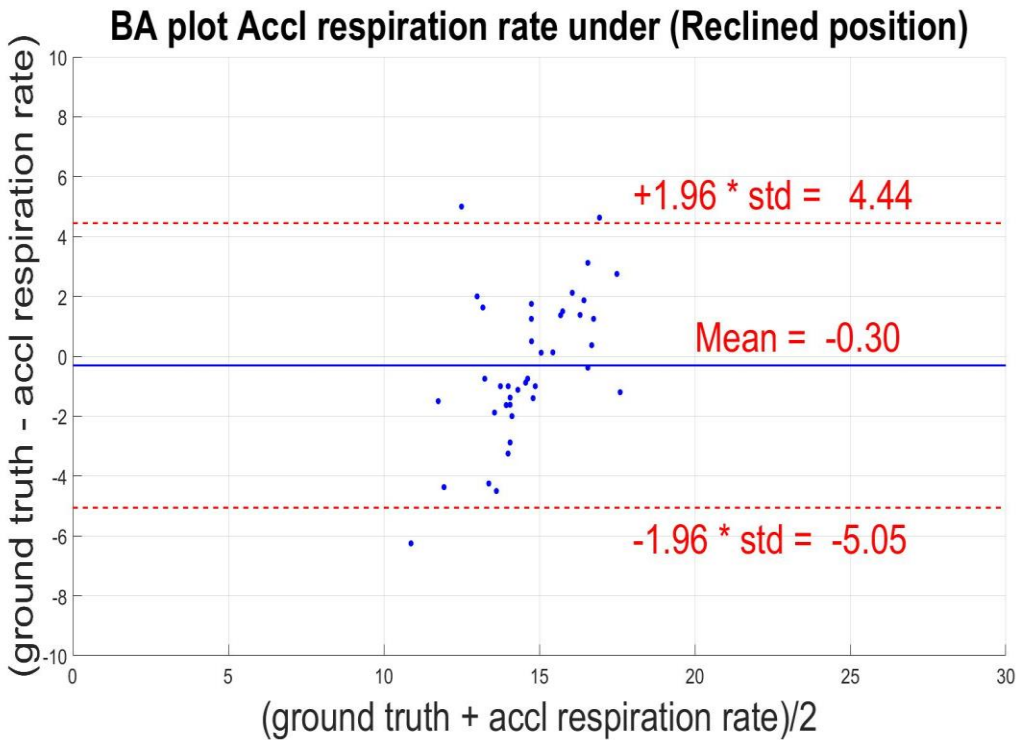

Figure 4.8: Bland Altman plot for the accelerometer placed under cushion and ground truth average respiratory rate in the reclined position.

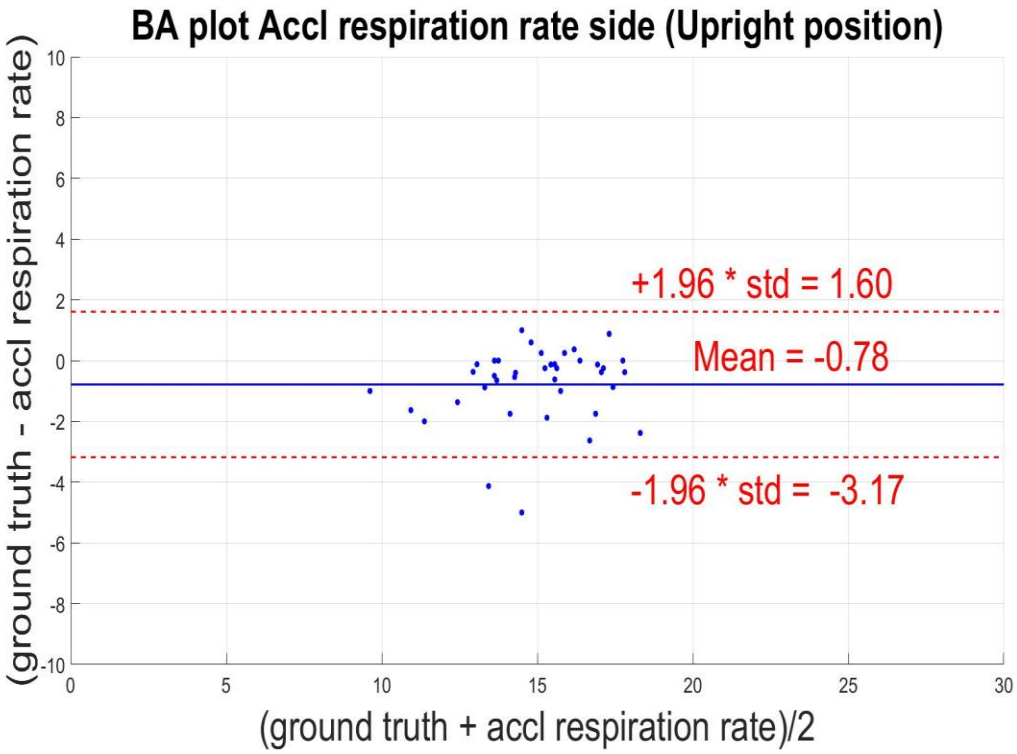

Figure 4.9: Bland Altman plot for the accelerometer placed side of the cushion and ground truth average respiratory rate in the upright position.

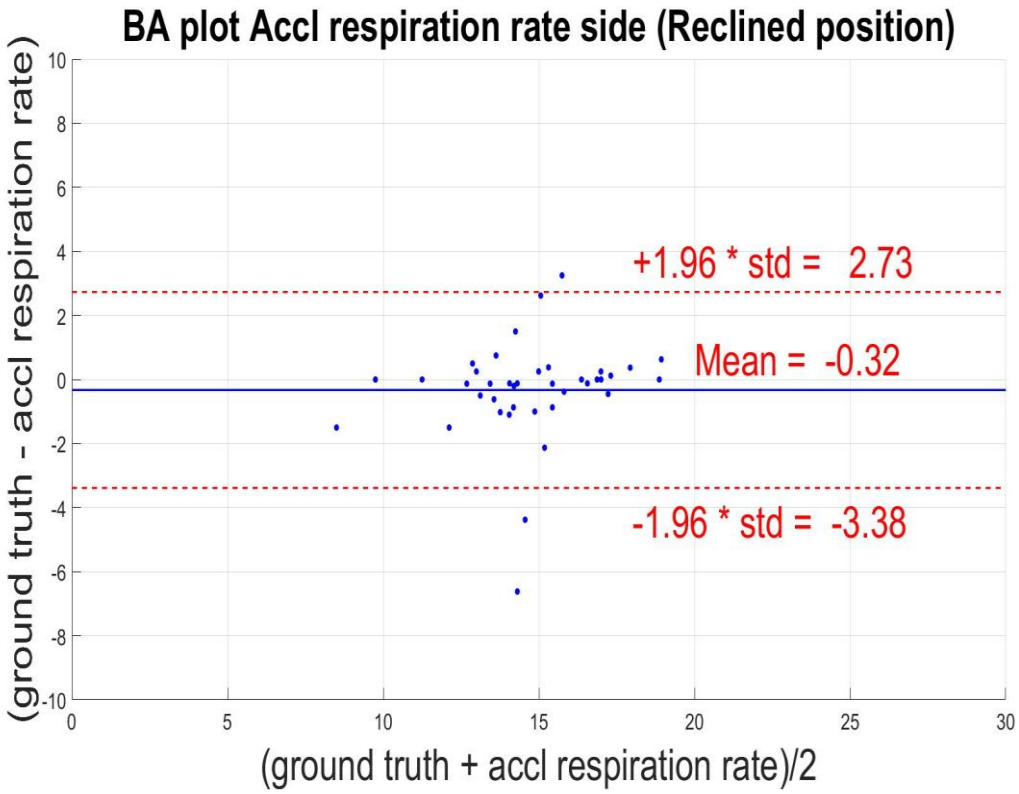

Figure 4.10: Bland Altman plot for the accelerometer placed side of the cushion and ground truth average respiratory rate in the reclined position.

4.3 Linear plot graphs

These graphs are plotted to analyse how well the heart and respiration rates obtained from the chair sensor track or linearly follow the ground truth values. On the x-axis we plot the ground truth heart rate/respiration rate and on the y-axis we plot the accelerometer heart rate/respiration rate corresponding to the same subject. Once these values are plotted then the reference line of the ground truth (red) is drawn for comparison purposes. Like the BA plot, There are 4 plots for the heart rate and 4 plots for the respiration, each having the results plotted for both the under and the side accelerometer, both in the upright and reclined positions. Table 4.2 shows the correlation coefficient values for these chair and accelerometer combinations.

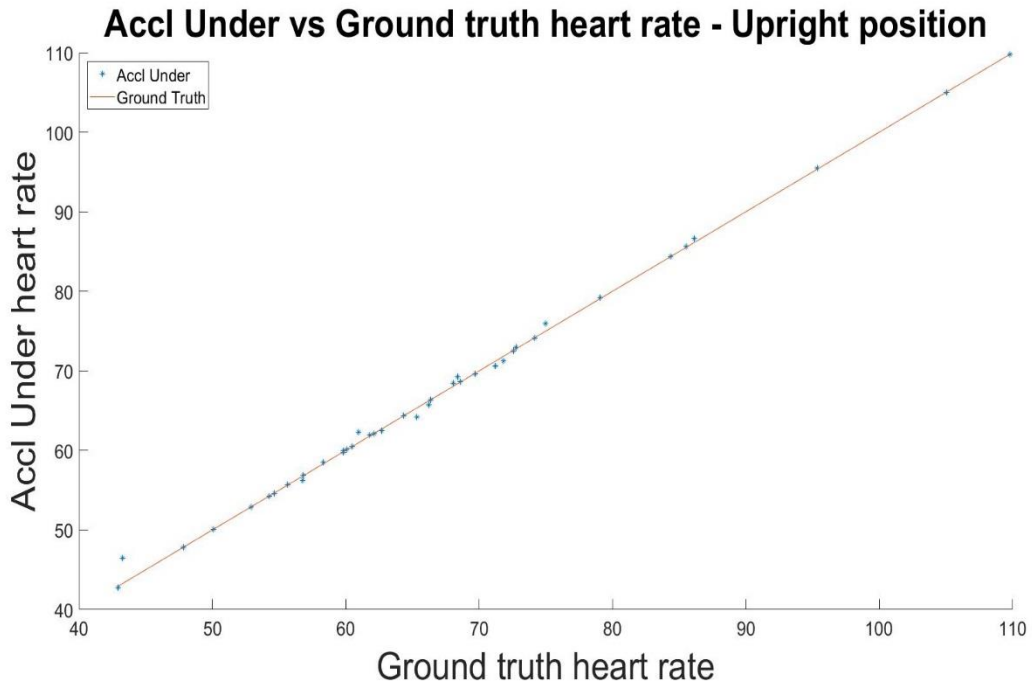

Figure 4.11: Plot of the ground truth and accelerometer (under) heart rate for the study subjects in the upright position. Note the ideal case (red) shown for reference.

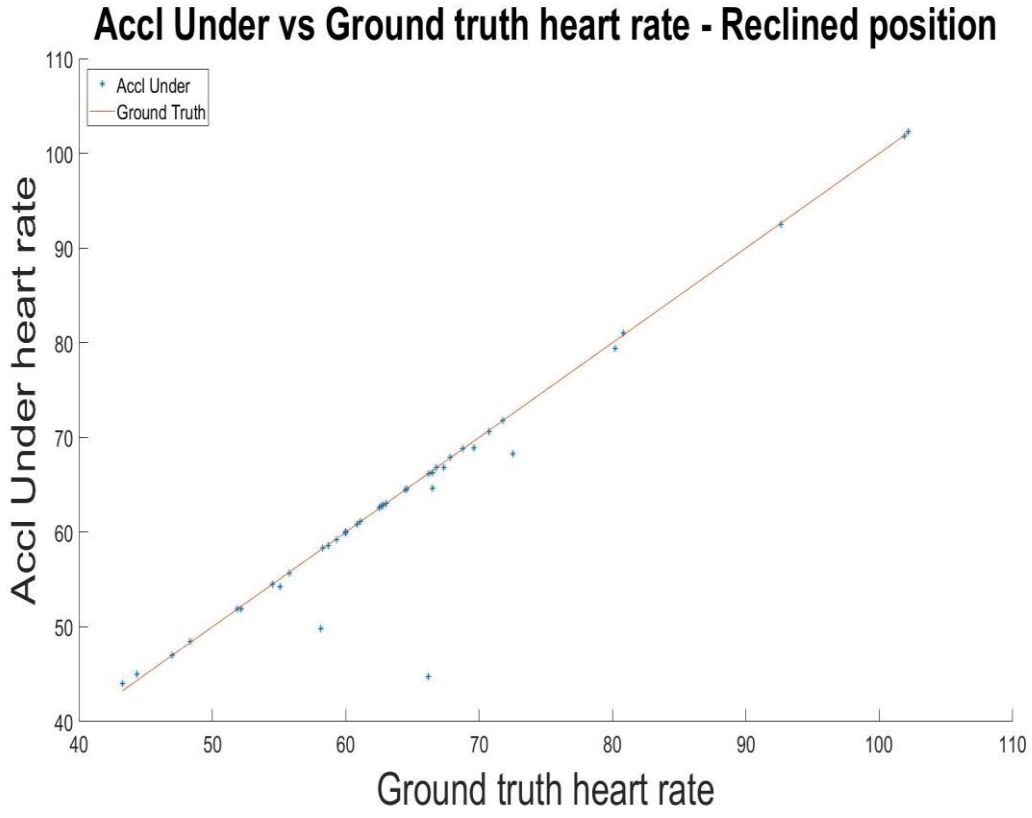

Figure 4.12: Plot of the ground truth and accelerometer (under) heart rate for the study subjects in the reclined position. Note the ideal case (red) shown for reference.

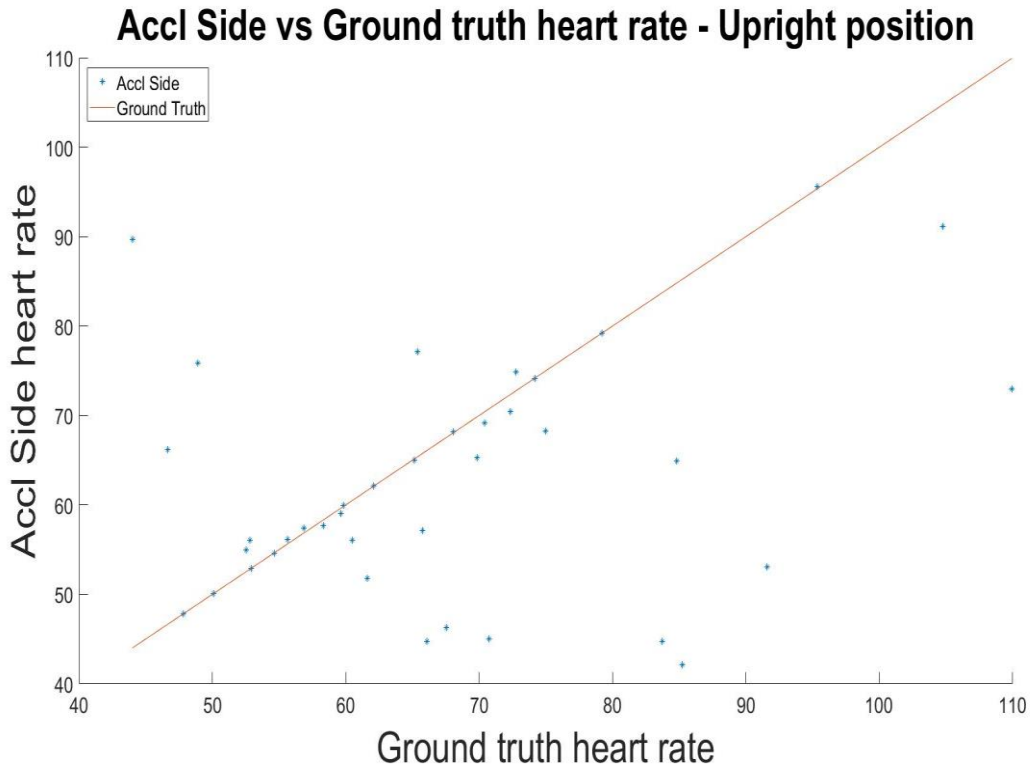

Figure 4.13: Plot of the ground truth and accelerometer (side) heart rate for the study subjects in the upright position. Note the ideal case (red) shown for reference.

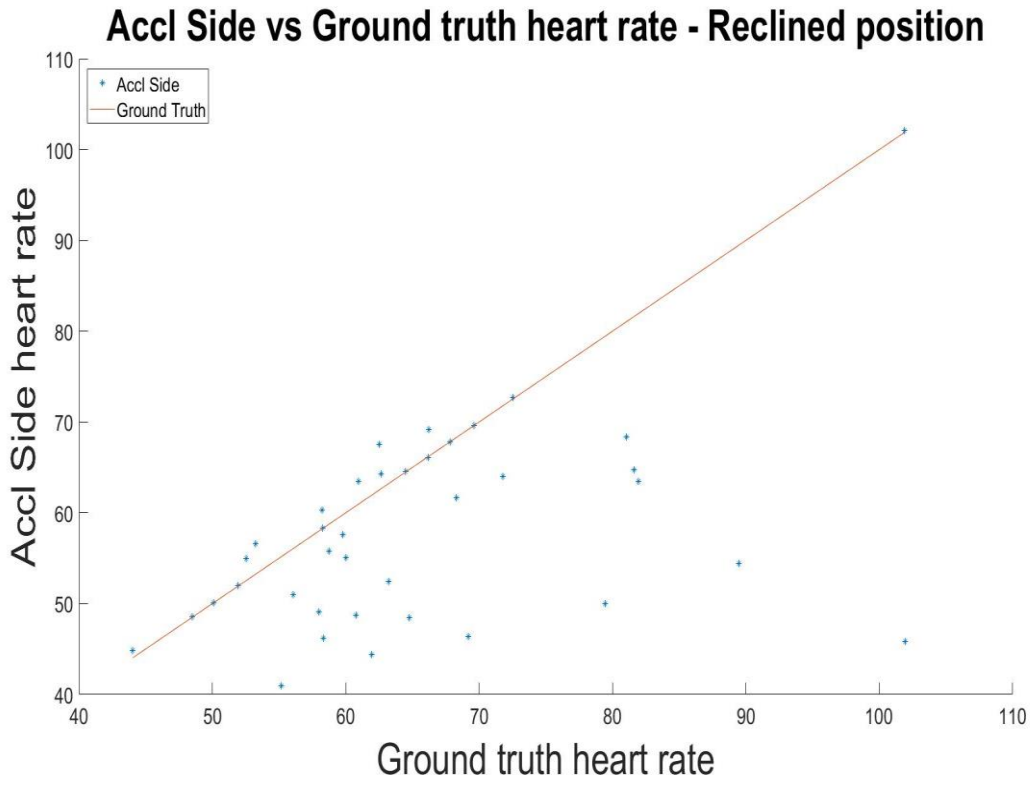

Figure 4.14: Plot of the ground truth and accelerometer (side) heart rate for the study subjects in the reclined position. Note the ideal case (red) shown for reference.

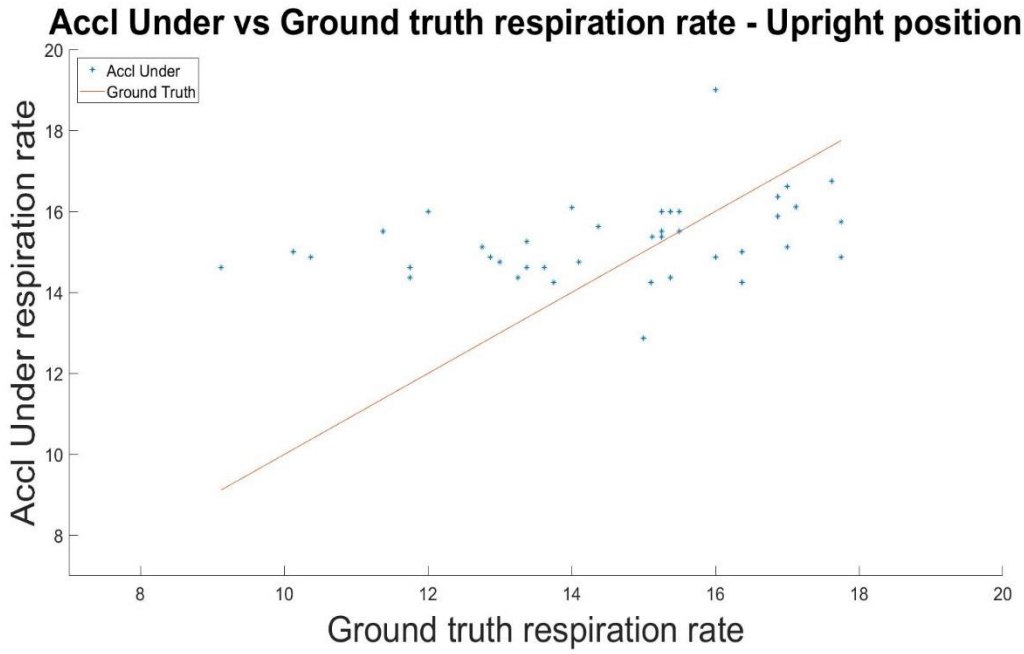

Figure 4.15: Plot of the ground truth and accelerometer (under) respiratory rate for the study subjects in the upright position. Note the ideal case (red) shown for reference.

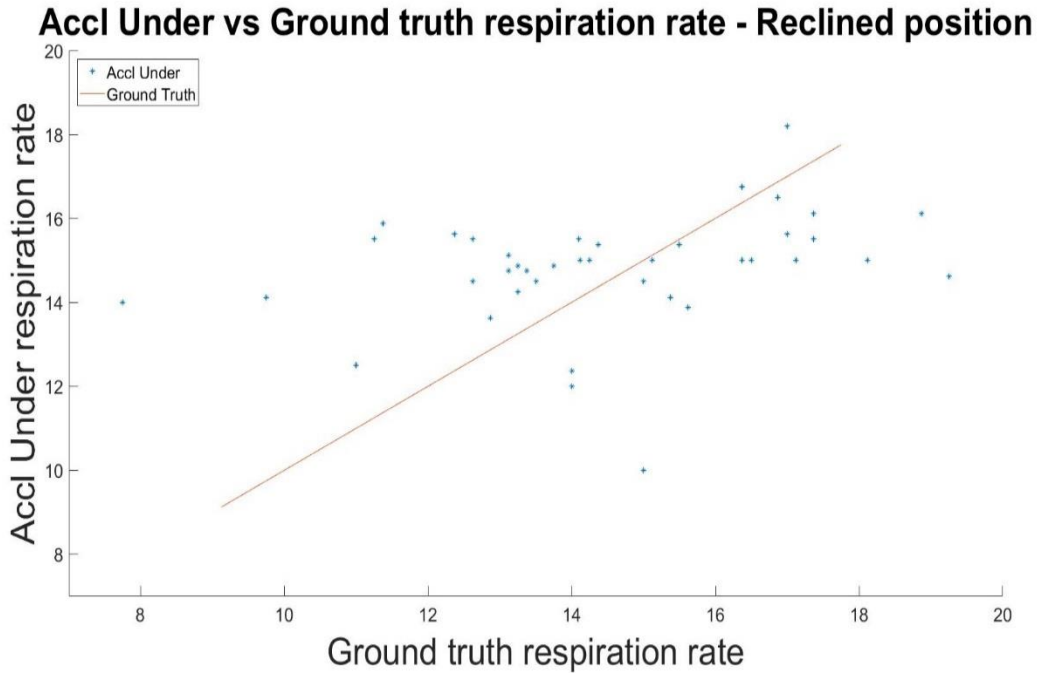

Figure 4.16: Plot of the ground truth and accelerometer (under) respiratory rate for the study subjects in the reclined position. Note the ideal case (red) shown for reference.

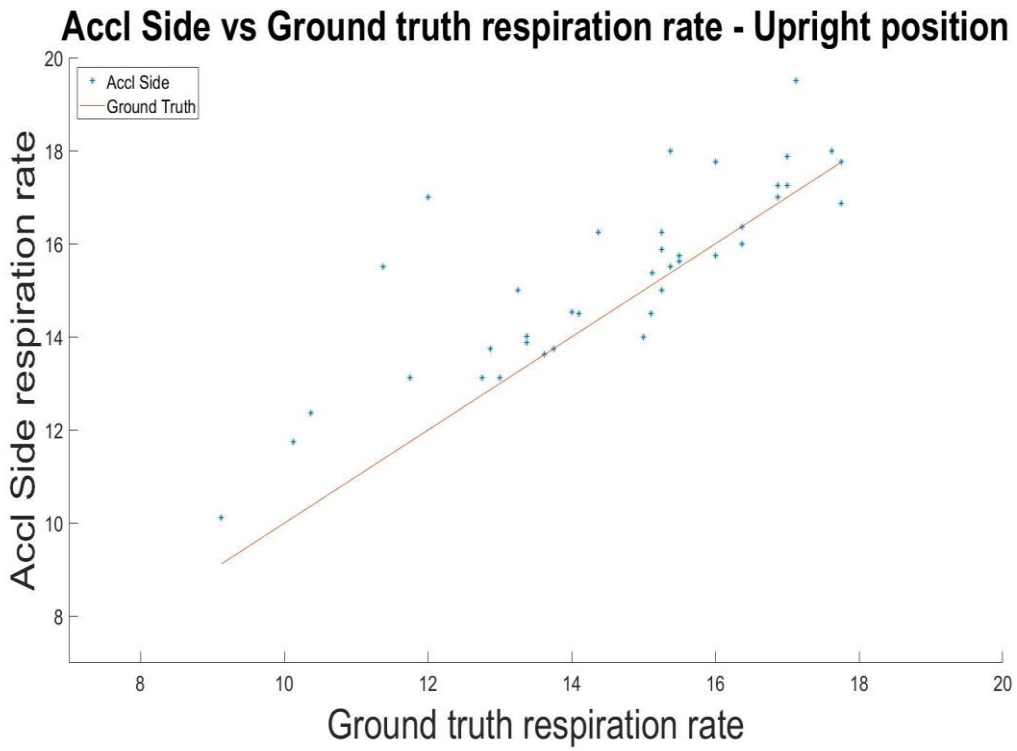

Figure 4.17: Plot of the ground truth and accelerometer (side) respiratory rate for the study subjects in the upright position. Note the ideal case (red) shown for reference.

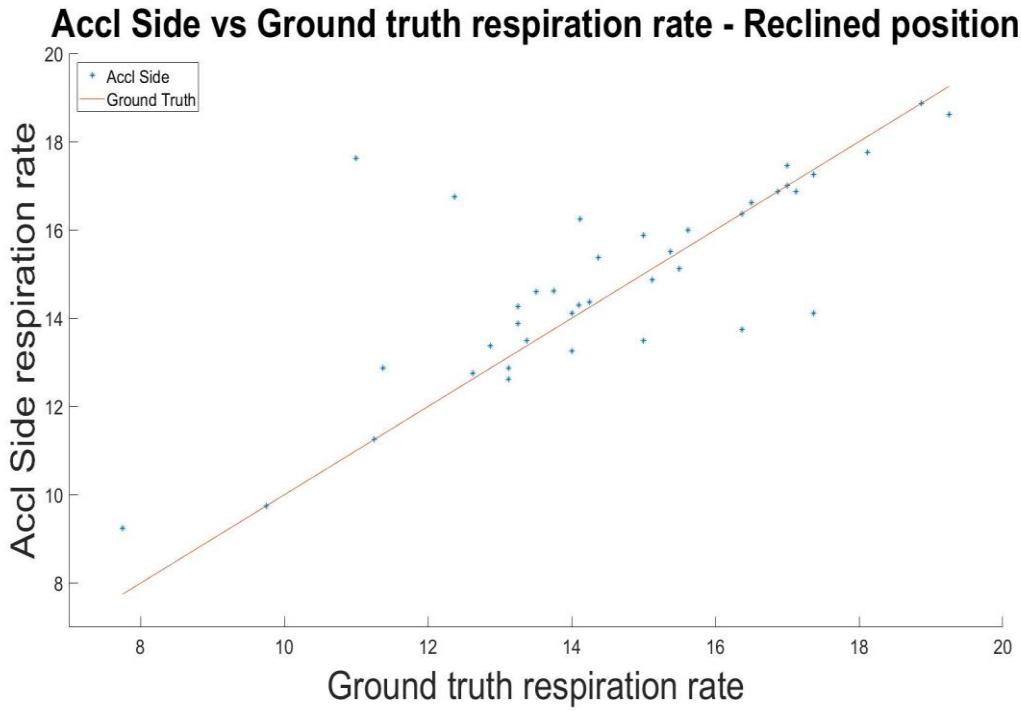

Figure 4.18: Plot of the ground truth and accelerometer (side) respiratory rate for the study subjects in the reclined position. Note the ideal case (red) shown for reference.

Parameter	Accelerometer Under – Up right	Accelerometer Under - Reclined	Accelerometer Side - Upright	Accelerometer Side - Reclined
Heart Rate	0.99	0.96	0.29	0.47
Respiratory Rate	0.34	0.30	0.83	0.78

Table 4.2: Accelerometer Correlation Coefficient - Heart and Respiratory Rate

Parameter	Average Upright	Average Reclined	Standard Deviation Upright	Standard Deviation Reclined
Heart Rate (beats/min)	67.02	64.68	14.76	12.9
Respiratory Rate (breaths/min)	15.29	14.81	1.98	2.20

Table 4.3: Study statistics heart rate (beats/min) - Accelerometer under, respiratory rate (breaths/min) - Accelerometer side.

4.4 Age and gender error rates

From the BA plot and correlation coefficient values it can be seen that the accelerometer placed under the recliner gives more accurate results for the heart rate and the accelerometer on the side of the cushion gives more accurate results for the respiration rates. Hence our system reports these values from the respective accelerometers. Correspondingly error rates for these accelerometers values are shown below. The errors shown in the Table 4.4 and Table 4.5 are average percentage error rates. They are calculated by calculating the individual subject percentage error rate between the accelerometer and the ground truth, then classifying these according to the age and gender and taking the average of these percentage errors. We get a slightly inflated number for the respiration errors since typical respiration rates lie between 12 - 20 breaths/min for an average person compared to heart rates values of 40 - 100 beats/min. It has to also be kept in mind that the number of subjects in each category

are not equal both in terms of age and gender, and we are limited by our data set. The study subject age and gender distribution is shown in Table 3.2.

Age (years)	Male (%)	Female (%)	Total (%)
55 - 60	0.03/0.09	0.26/0.08	0.18/0.09
61 - 70	0.09/0.01	0.20/0.09	0.19/0.08
71 - 80	0.70/0.11	0.81/0.09	0.75/0.10
81 - 90	0.09/2.90	0.57/4.50	0.44/4.20
91 - 100	0.52/0.48	1.67/0.86	1.16/0.70
Total	0.41/0.61	0.68/1.49	0.59/1.37

Table 4.4: Heart rate average percentage error - Accelerometer under (upright/reclined)

Age (years)	Male (%)	Female (%)	Total (%)
55 - 60	2.90/0.51	6.61/6.24	5.39/2.20
61 - 70	6.50/2.45	7.10/6.99	7.02/6.34
71 - 80	13.57/14.06	5.37/0.93	9.47/7.50
81 - 90	12.07/4.48	3.84/4.46	5.21/4.47
91 - 100	11.40/16.25	6.05/7.24	9.39/12.87
Total	10.56/10.71	5.45/4.61	7.19/7.08

Table 4.5: Respiratory rate average percentage error - Accelerometer side (upright/reclined)

4.5 Correlation variations - Different confidence levels

In [5], where the HT Algorithm is described, a confidence level of 25k is suggested. It is important to have a confidence level for the HT Algorithm, since it relies on the approximation that the noise is low. This is required for equation (4) to be valid. One of the methods to test how effective the HT Algorithm is in filtering the noisy signals is to gradually lower the confidence level and check if the correlation coefficient proportionately decreases. This should happen because as the confidence is lowered the noisier signals are added while calculating the correlation bringing down the overall value. This is exactly what we have tested for. Figure 4.19 and Figure 4.20 show the correlation values for different confidence levels. A confidence of 0 implies that no confidence is applied and we just take the output from the HT algorithm.

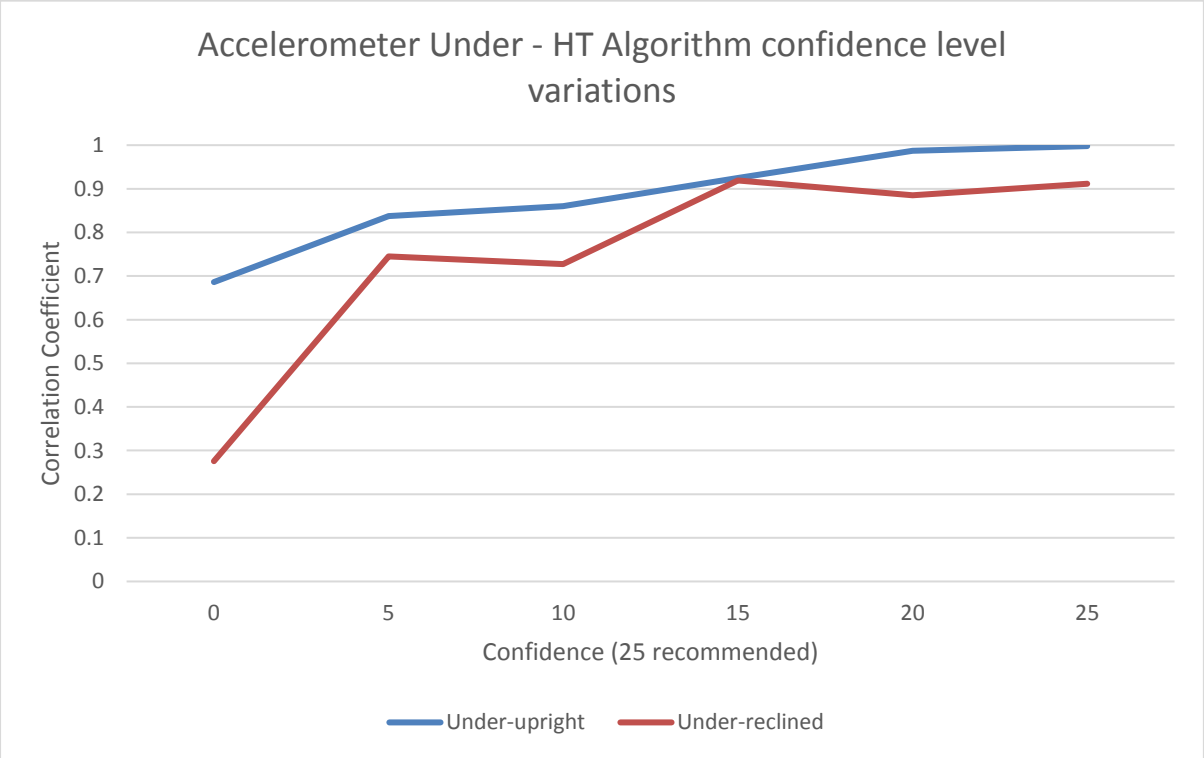

Figure 4.19: Plot of the HT algorithm average heart rates for various confidence levels for the accelerometer placed under the seat cushion.

Figure 4.19 shows the trend for the correlation coefficient values for calculating the heart rate when the accelerometer is placed under the chair. Both configurations of reclined and upright are tested. It can be seen that the upright correlation values have a much smoother increase than the reclined values. In fact this is what we observe even in the error rates with the upright configuration giving the least error. Figure 4.20 shows the same type of plot, but for the accelerometer placed on the side of the seat cushion. It is to be noted that we do not consider the values for the heart rate (in the final system) from the side accelerometer and the values in Figure 4.20 are just used for a comparison. When the confidence level is low the reclined configuration has a higher correlation but this trend reverses at the recommended confidence level of 25k. It cannot be said with certainty that the reclined configuration is better for the side accelerometer because most of the signals at lowered confidence level are noisy and the trend may be attributed to randomness.

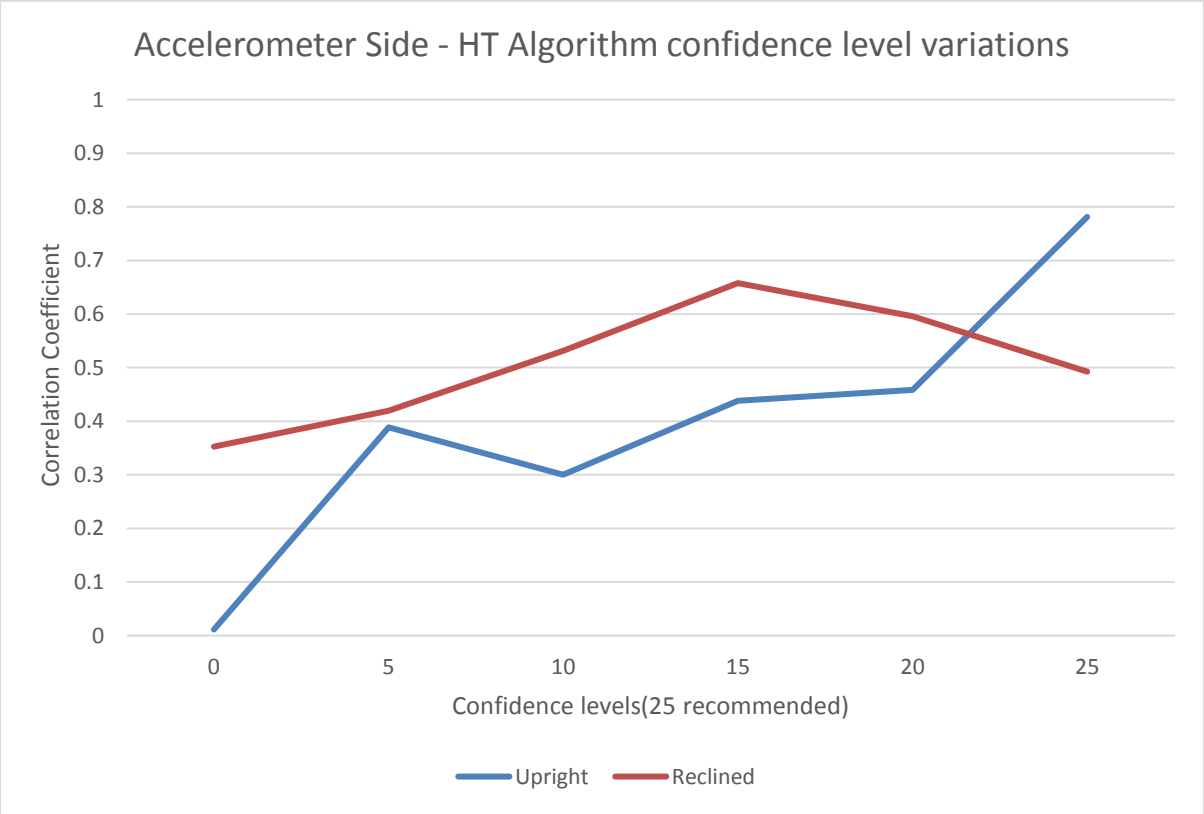

Figure 4.20: Plot of the HT algorithm average heart rates for various confidence levels for the accelerometer in the side position.

Confidence	Correlation Coefficient - Upright position	Correlation Coefficient- Reclined position
0	0.68	0.27
5	0.83	0.74
10	0.86	0.72
15	0.92	0.88
20	0.98	0.911

Table 4.6: Correlation Coefficient for the upright and reclined positions (accelerometer side) with varying confidence levels used in the HT Algorithm.

Confidence	Correlation Coefficient - Upright position	Correlation Coefficient- Reclined position
0	0.01	0.35
5	0.38	0.41
10	0.30	0.53
15	0.43	0.65
20	0.45	0.59

Table 4.7: Correlation Coefficient for the upright and reclined positions (accelerometer under) with varying confidence levels used in the HT Algorithm.

4.6 Murata SCA11H results

4.6.1 Processed Data Mode

In the processed data mode, the sensor outputs the heart rate and respiration rate values every second. Our accelerometer on the other hand gives continuous values of the signal. Hence we calculate the beat to beat interval and the breath to breath interval of the obtained signal from our accelerometer, and from those intervals we can calculate the instantaneous heart and respiration rates. We had collected the data for about 10 minutes. We then take the median of these values to compare between the Murata and our sensor system. Table 4.8 shows the values obtained for the heart rate. Similarly Table 4.9 shows the results for the respiration rate.

Parameter	**Median Heart rate (beats/min)**
PPG Sensor	85.71
Accelerometer Under	85.71
Murata Sensor Under (processed mode)	82

Table 4.8: Comparison between the accelerometer and the Murata SCA11H (tested in processed mode) heart rate both tested under the cushion of the chair.

Parameter	**Median Respiratory rate (beats/min)**
Chest Band	21.05
Accelerometer Side	20.47
Murata Sensor Side (processed mode)	11

Table 4.9: Comparison between the accelerometer and the Murata SCA11H (tested in processed mode) respiratory rate both tested on the side cushion of the chair.

4.6.2 Raw Data Mode

In the raw data mode, the Murata sensor outputs the data obtained from the accelerometer in hexadecimal format. Here also the data was collected for about 10 minutes.

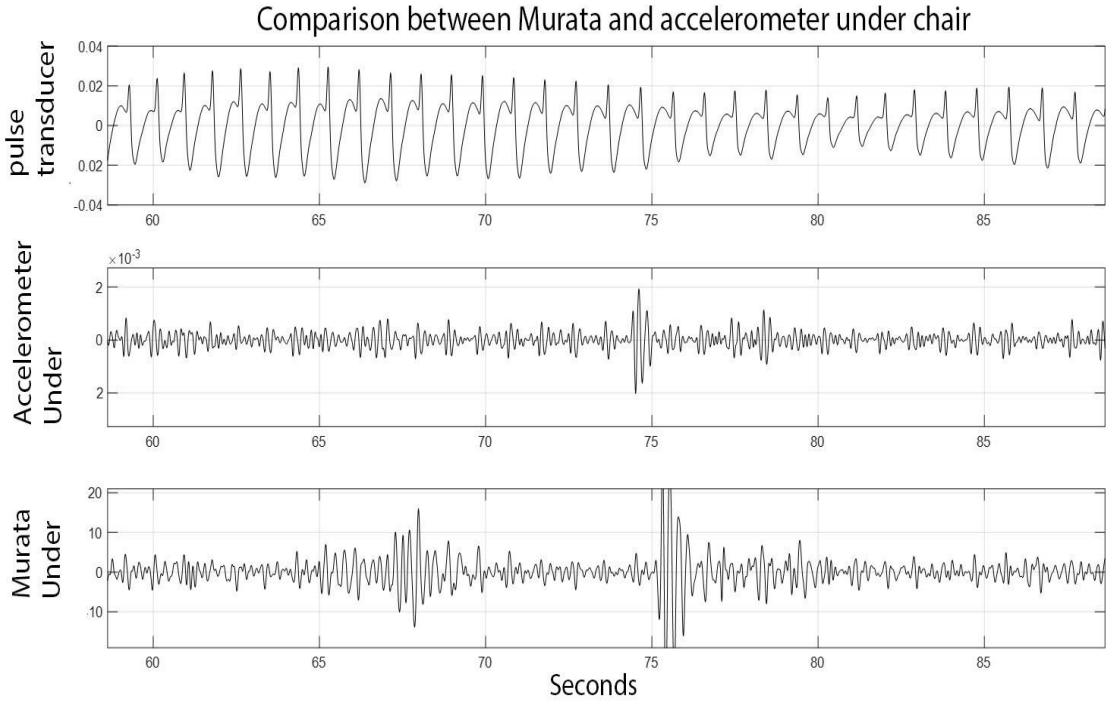

Figure 4.21: Comparison between the heart signal obtained from the pulse transducer (ground truth), the accelerometer and the Murata SCA11H (raw data mode) placed under the cushion.

Parameter	HT Algorithm average heart rate (beats/min)
PPG Sensor	74.54
Accelerometer Under	73.96
Murata Sensor Under (raw mode)	74.96

Table 4.10: Comparison between the accelerometer and the Murata SCA11H (tested in raw data mode) heart rate, both tested on the side cushion of the chair.

Figure 4.21 shows the heart rate signals obtained from the pulse transducer (ground truth), accelerometer and the Murata sensor. Note a disturbance is provided for

synchronization in Figure 4.21. Table 4.10 shows the HT Algorithm average heart rate values for all the 3 sensors. Figure 4.22 shows the signals obtained when the accelerometer and the Murata sensor are placed on the side of the cushion. Both the sensors output noisy signals. When we compare the respiration rate, we find that the Murata sensor is unable to accurately give signals from both the under and the side accelerometer.

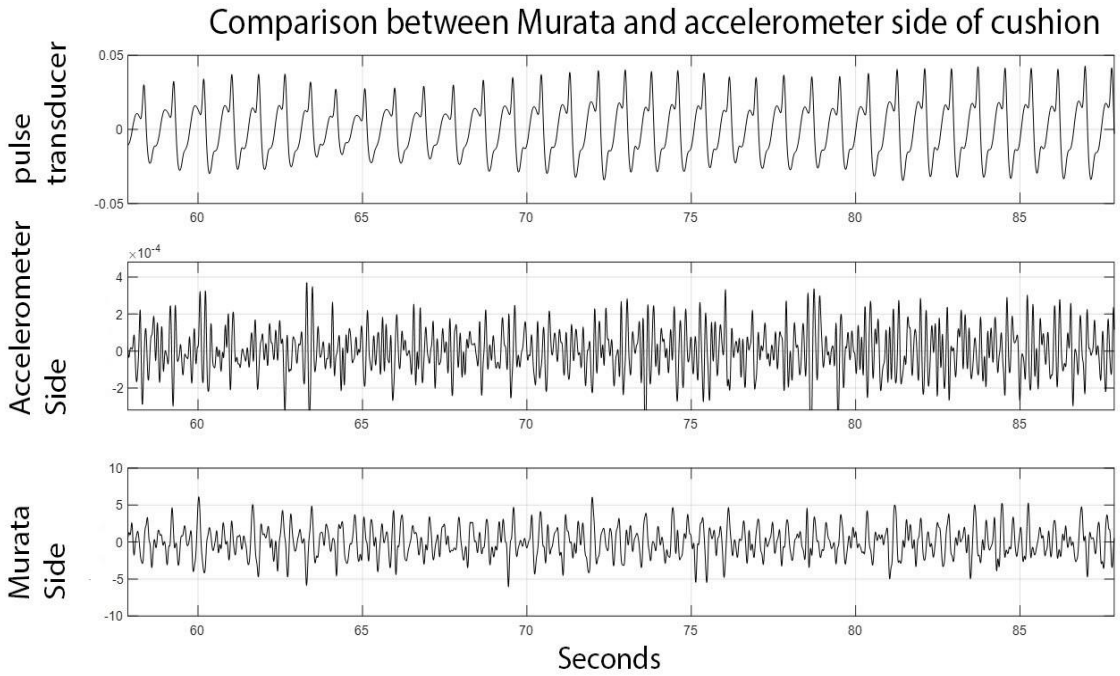

Figure 4.22: Comparison between the heart signal obtained from the pulse transducer (ground truth), the accelerometer and the Murata SCA11H (raw data mode) placed on the side of the cushion.

Parameter	**Median Respiration rate (breaths/min)**
PPG Sensor	19.7
Accelerometer Under	19.94
Murata Sensor Under (raw mode)	14.3

Table 4.11: Comparison between the accelerometer and the Murata SCA11H (tested in raw data mode) respiration rate, both tested on the side cushion of the chair.

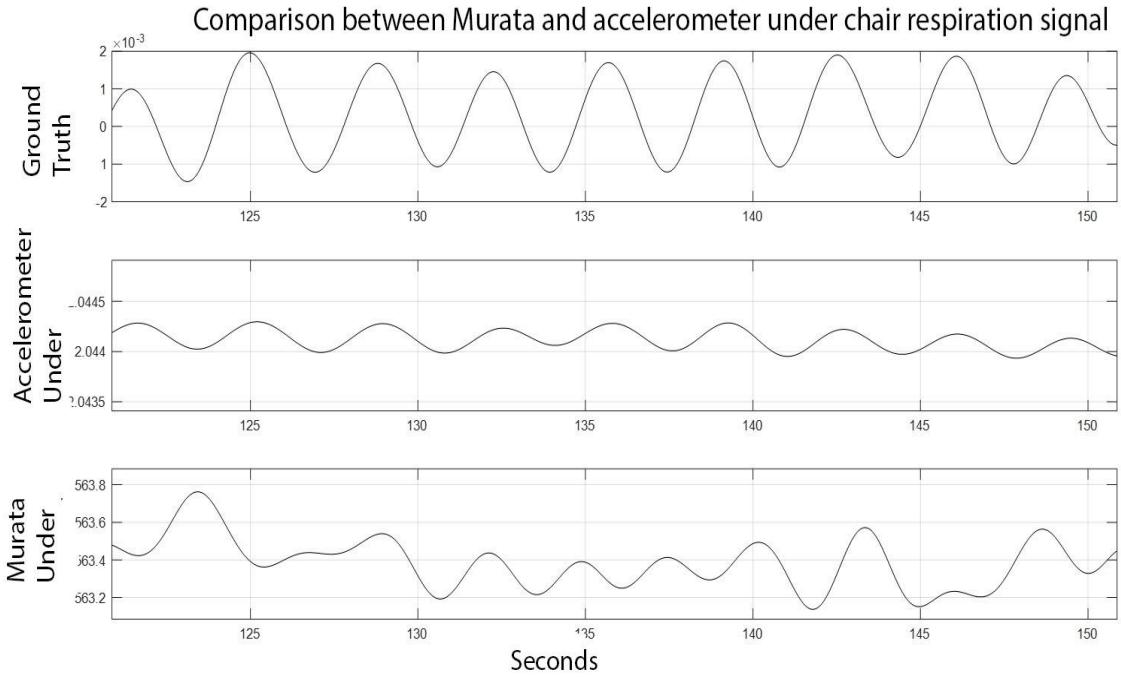

Figure 4.23: Comparison between the respiratory signal obtained from the chest band (ground truth), the accelerometer and the Murata SCA11H (raw data mode) placed under the cushion.

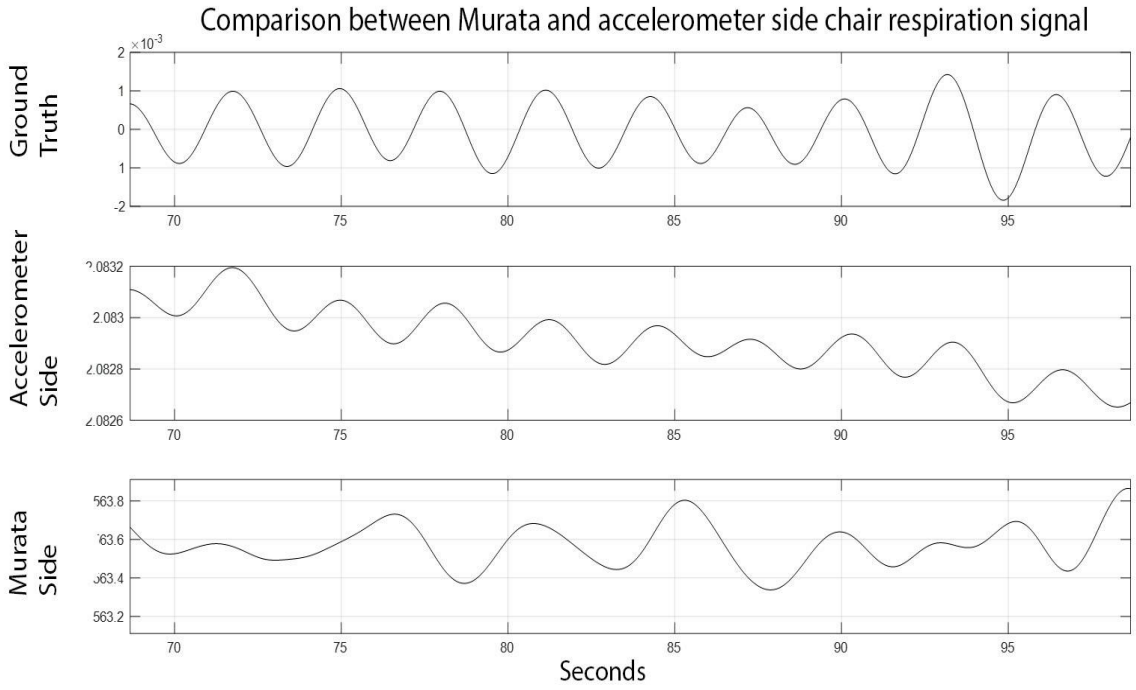

Figure 4.24: Comparison between the respiratory signal obtained from the chest band (ground truth), the accelerometer and the Murata SCA11H (raw data mode) placed on the side cushion.

4.7 BPI results - Chair study subjects

The Breathing pattern Index (BPI) was applied to the respiration data obtained from the chair sensor. The data collected from the side accelerometer was used in this case. The subjects were divided into 3 categories, i.e. subjects who were healthy, had lung problems and subjects who had heart problems. Healthy subjects are those who had all negative answers (except drank coffee) in the questionnaire that was asked to be filled before conducting the test for every subject. Similarly heart and lung problem subjects are the ones who had the affirmative for the respective questions. It has to be noted that, these classifications are made based on what the subject answered while conducting the study. This data was not obtained from their medical records, and it could be likely in some cases (though rare) the subject may have incorrectly answered a question about their health conditions. The average age of the subjects who participated was 78.8 years.

Subject ID	**Median BPI**	**Respiration Rate (breaths/min)**
1235	0.48	11.62
1205	0.89	16.25
1212	0.19	17.25
1222	0.41	16
1228	0.58	13.75
1230	0.20	10
1234	0.58	12.25
1242	0.19	11.25

Table 4.12: Median BPI for the healthy chair study subjects. The values tend to be on the lower side (roughly below 0.6).

Subject ID	Median BPI	Respiration Rate (breaths/min)
1207	1.30	12.87
1227	0.80	16.25

Table 4.13: Median BPI for the chair study subjects with lung problems. The values tend to be on the higher side.

Subject ID	Median BPI	Respiration Rate (breaths/min)
1204	1.32	13.7
1206	0.52	16.2
1207	1.30	12.8
1208	2.8	16.7
1213	0.98	14.5
1214	0.75	16.8
1215	0.2	12.8
1221	0.15	12.8
1223	0.82	14.6
1226	0.33	14.5
1227	0.92	16.2
1231	1.28	15.3
1237	0.64	13.25
1239	1.3	15.62
1241	0.62	12.7
1245	1.4	12.5

Table 4.14: Median BPI for the chair study subjects with heart problems.

Table 4.12 shows the BPI values for the healthy subjects Table 4.13 and Table 4.14 shows the BPI values for the lung and heart problem subjects respectively. Generally the healthy subjects tend to have values on the lower side. 1205 can be considered an outlier among the healthy subjects since the subject had a respiration rate of 18, which tends to also increase the BPI values. Similarly, there are 1-2 outliers in the heart problem subjects also.

Chapter 5

Discussion

5.1 Chair Sensor Study Results

Figure 4.3 – Figure 4.6 shows the Bland-Altman (BA) plots for results obtained from calculating the average percentage error for the heart rate. We can see that the plots for the accelerometer placed under the seat cushion gives more accurate results with the mean of the difference between ground truth and accelerometer (under) being -0.10 for the chair in the upright position and 0.93 for the chair in the reclined position. The 95% limit of agreement standard deviation values are much lower when the chair is in the upright position. Also overall the standard deviation for the accelerometer placed under is less when compared to the values in the BA plots shown for the side accelerometer in Figure 4.5 and Figure 4.6. For the plot shown in these figures a confidence of 10*k* was used. This is because using a 25*k* confidence for the side accelerometer will result in many null values (arbitrarily 0) due to noisy signals, artificially increasing the difference between the ground truth and side accelerometer values in the plot. This will cause a BA plot with very high standard deviation and bias. Hence to get a similar comparison between the two plots, the 10k confidence is used. The heart rate readings from the side accelerometer is not used in the real system and the plot is shown for comparison purposes only.

Table 4.2 shows the correlations for the different configurations. We can see that the side accelerometer has 0.29 and 0.47 correlation values for the upright and reclined positions, respectively, while the accelerometer placed under the chair has correlations of 0.99 and 0.96 for the upright and reclined configurations respectively. Hence we have decided to capture the heart rate estimate from the accelerometer placed under the seat cushion for our sensor system.

The lowest heart rate recorded in the study was about 43 beats/minute for a 91 year old female. The highest heartrate recorded was 109 beats/minute for a 62 year old female.

On the whole the heart rate estimate is quite accurate for the accelerometer placed under the cushion even in terms of the average percentage error, as we get 0.59% and 1.37% error for the upright and reclined positions respectively. The results include both healthy and non-healthy subjects. The average heart rate of the subject population was 67.02 heartbeats per minute. It can be noticed from Table 4.4, that the average percentage error for the heart rate increases when the chair is in the reclined position. This is in agreement with Ballistocardiogram (BCG) signal analysis. When the chair is in the upright position, most (if not all) of the body's reaction forces are acting upon the seat of the chair, since this is the part of the chair that is in most contact with the body. Our accelerometer is placed directly under the cushion of the chair, which comes directly under the gluteus muscles of the occupant. Hence the accelerometer captures the maximum force when compared to the reclined position. In the reclined position, the body is in contact with both the backrest, and the seat of the chair, depending on the angle of recline. The height and the mass distribution can also play a role with the accuracy of the heartrate obtained when the chair is in the reclined position. For example if a person has most of his mass distribution on the upper parts of the body, then we are likely to see a larger error from the accelerometer placed under the cushion, because most of the reaction forces will act on the backrest of the chair. Although there is an increase in error for the chair in the reclined position, it is minimal, and the overall error calculated for all the subjects is about 1.37% as shown in Table 4.4.

It can also be seen from the Table 4.3 that the average heartrate of all the subjects in the upright position is 67.02 and in the reclined position is 64.68. This is because, in the reclined position the occupants are more likely to take a nap, and hence be more relaxed lowering the average heartrate. One other plausible reason could also be the order of testing, i.e. the occupants were always first tested in the upright position. At TigerPlace assisted living the study was conducted in a small hall, and the subjects had to walk from their rooms to the study location. Considering the area of the assisted living facility, on average a person had to walk at least 400 m to reach the study site. And when the participants arrived at the site, they were seated on the recliner chair in the upright position and their data began recording after 1 minute. Considering the average age (78.8 years) of the participants, walking would constitute a considerable

amount of exercise, which may explain the increase in the average heartrate for the upright position. Since the reclined data was collected after 15 minutes in the upright position, their heartrate may have slowed down. A similar trend can be seen in the standard deviation for the reclined and upright positions. Considering the age variations (98-oldest, 56- youngest) and the walking-exercise factor, it would be plausible to assume that the standard deviation for the upright position to be higher. From the Table 4.3 it can be seen that for the upright position it is 14.76 and the reclined position it is 12.9 heartbeats.

The performance is flipped when it comes to respiration, as the side accelerometer performs accurately hence the requirement for both the accelerometer. Only the z-axis data of the accelerometer is required to accurately predict the heart and respiration rates and hence the system remains quite simple with only 2 channels required.

5.1.1 HT Algorithm Average Error Rates According to Gender and Age

Before we make conclusions regarding any specific general trend, we have to consider the male/female distributions of our dataset. We had tested the recliner chair on 14 males and 31 females as shown in Table 3.2. Table 4.4 shows the average percentage error rate according to age and gender. We can see that the error rate increases as the subjects get older, with 91 – 100 years age group having an error percentage of 1.1 %. This is expected because the heart muscles get weaker with age and hence the reaction forces are also of a lower magnitude. Not only that, older people also tend to have more heart related problems, making them have a noisier signals (or reaction forces). In a study conducted in [30], about changes in heart function parameters with age, it has been reported that with age there is a deterioration in Left ventricular mass (LVM), End diastolic volume (EDV), End systolic volume (ESV) and Ejection fraction (EF). For example, the Ejection fraction quantifies the amount of blood pumped out of the heart with each contraction. We know from [30] that elders generally tend to have a lower EF. The major causes of low ejection fraction are Coronary artery disease and heart attacks. We had many heart attack patients tested on our recliner chairs which could explain the slight decrease in accuracy. Generally patients with clogged and narrow arteries have

less accuracy, since the reaction forces obtained from the contraction and expansion of the heart muscles are not cleaner, in other words they tend to be more complex in shapes, which results in their signals spread across multiple frequencies, giving less accurate results when the HT Algorithm is applied. From Table 4.4 we can also see that the male percentage error is low when compared to females. We cannot state this as a general trend because of our skewed data set (14 males, 31 females), but in the 71 – 80 years age group category we had 4 males and females and the average male percentage error is lower. This may be the case, due to on average the male heart being 1/3 (about 60 grams) times larger than that of females, and hence resulting in stronger reaction forces captured by the accelerometers. The correlation values are shown in Table 4.2. They follow a similar trend as the error rate values.

5.1.2 Respiration Rate discussion

Figure 4.7 – Figure 4.10 shows the BA plot obtained for the average respiration rate calculated from the accelerometers. Although the BA plots show similar mean and standard deviations for all 4 configurations, the average values (x-axis) for the under seat cushion accelerometer vary very little. This means that the under accelerometer is picking low frequency noise rather than the respiration signal. This can be clearly seen in the correlation values obtained in Table 4.2 where 0.34 and 0.3 are obtained for the under accelerometer while 0.83 and 0.78 are obtained for the side accelerometer for the upright and reclined positions, respectively. Hence we choose the accelerometer values from the side of the seat cushion to report respiratory rate. Therefore two accelerometers are required to accurately estimate heart and respiratory rates. The lowest respiration rate obtained during our study was 10 breaths/min, from a 64 year old female diagnosed with sleep apnea. The highest was 18 breaths/min from a 79 year old male subject. The average percentage error rate of around 7% was obtained for both the subjects in the upright and reclined position. The average respiration rate for the upright position is 15.3 with the standard deviation of 1.98 breaths/min. As can be seen from Table 4.3, the average respiration rate for the subjects in the reclined position is 14.8, with a standard deviation of 2.2, or about 2.6% less when compared to the upright position. This can be explained by the order of testing for the upright and reclined positions as explained previously.

5.2 Murata SCA11H comparison results

We can see from Table 4.8, 4.9 and 4.10 that the Murata sensor heart rate is quite consistent with the readings of the accelerometer and the ground truth. Figure 4.21 shows the heart signal obtained from the Murata sensor in the raw data mode. Although the J peaks cannot be clearly distinguished from a visual point of view, the HT Algorithm output is accurate with respect to the ground truth as shown in Table 4.10. The Murata sensor however underestimates the respiration rate, both in the raw and processed data modes. This may be because the Murata sensor does not calculate the respiration rate directly by detecting the peaks from the signal obtained in the raw data mode.

The Murata sensor only measures the true heart pumping signal or the BCG signal, and all the other parameters such as Heart rate, Respiratory rate, Heart rate variability, and relative stroke volume are calculated from this signal using their software algorithms. Thus respiration rate outputted by the sensor is only an indirect measure. The respiration rate is specifically extrapolated from the periodical changes in the stroke volume and beat to beat intervals caused by the respiration. In [45], it is shown that with the onset of inspiration, the mean stroke volume fell by 7% and during expiration there was an increase. This has an effect on the beat to beat intervals from which the amount of change in respiration is measured. Therefore, if we do not get a very clean BCG signal, the accuracy of all the other parameters will also suffer. This may be the cause of the Murata sensor being unable to give accurate reading of respiration rates when tested on the chair.

Chapter 6

Conclusions and Future Work

6.1 Conclusions

In this work a non-invasive sensor system that captures vital signs is developed for use in recliner chairs. The location of the accelerometers (sensors) placed on the recliner chair was based on the requirements for older adults. Two accelerometers are used, one under the seat cushion to calculate the heart rate and another placed on the side of the seat cushion to calculate the respiration rate. The sensor system was tested with 45 subjects, with an average age of 78.8 years, on both the reclined and upright positions of the recliner chair. The sensor system works accurately in both cases with an error rate of about 1% for heart rate and 7% for respiration rate. Our sensor system will help in non-invasively monitoring of older adults vital signs, especially at night when they sleep in their recliners. However, there is one limitation, which we are currently working to solve. Since, our sensor system relies on capturing the movement caused due to the reaction forces from the body, the signals will get corrupted if the recliner chair has a rocking motion. Although the rocking motion is periodic, there are different types of rocking and it is highly dependent on the chair design. The results from the Murata SCA11H can give quite accurate heart rate estimated from the chair, however a reliable respiratory estimate could not be obtained. The results from the Breathing Pattern Index suggest that higher median BPI over time is indicative of poor respiratory health and lower median BPI indicates healthier breathing patterns.

6.2 Future Work

We are able to obtain a clean heart and respiration signal from the recliner chair. The next step would be to develop an embedded system that can be deployed at TigerPlace senior housing site to capture the signal data of older adults. Here we can assess how much we could improve our predictability of emergencies with the newly acquired data.

We are also working on developing diagnostic algorithms based on the morphology of the heart and respiration signals obtained from the chair sensor system. This means we are planning to predict health changes of the patient based on how much the shape of their signals change. We also are investigating how the BPI changes over time especially for patient diagnosed with Congestive Heart Failure (CHF).

Bibliography

[1] T. Y. Warren, V. Barry, X. Sui and S. P. Hooker, "Sedentary Behaviors Increase Risk of Cardiovascular Disease Mortality in Men," *Med. Sci. Sports Exerc.*, vol. 42, no. 5, pp. 879-885, May 2010.

[2] M. Rantz, M. Skubic, and S. Miller, "Using sensor technologies to augment traditional healthcare," in *Proc. 31st Annu Int. IEEE Eng. Med. Biol. Soc. Conf.*, Minneapolis, USA, Sept. 2009, pp. 6159-6162.

[3] Centers for Disease Control and Prevention (CDC), Healthy places terminology, Centers for Disease Control, Atlanta, GA, 2013. Available at: http://www.cdc.gov/healthyplaces/terminology.htm .

[4] D. Heise and M. Skubic, "Monitoring pulse and respiration with a noninvasive hydraulic bed sensor," in *Proc. 32nd Annu Int. IEEE Eng. Med. Biol. Soc. Conf.*, Buenos Aires, Sept. 2010, pp. 2119-2123.

[5] L. Rosales, B. Y. Su, M. Skubic and K. C. Ho, "Heart rate monitoring using hydraulic bed sensor ballistocardiogram," *J. Amb. Intel. Smart. En.*, vol. 10, pp. 193-207, Feb. 2017.

[6] I. Starr, A. J. Rawson, H. A. Schroeder and N. R. Joseph, "Studies on the estimation of cardiac output in man and of abnormalities in cardiac function, from the heart's recoil and the blood's impact; the ballistocardiogram," *Am. J. Physiol.*, vol. 127, no. 1, pp. 1-28, Aug. 1939.

[7] H. Rashvand, V. T. Salcedo, E. M. Sanchez and D. Iliescu, "Ubiquitous wireless telemedicine," *IET Commun.*, vol. 2, no. 2, pp. 237-254, Feb. 2008.

[8] R. R. Fletcher, M. Z. Poh and H. Eydgahi, “Wearable sensors: Opportunities and challenges for low-cost health care,” in *Proc. 32nd Annu Int. IEEE Eng. Med. Biol. Soc. Conf.*, Buenos Aires, Sept. 2010, pp. 17631766.

[9] A. Pantelopoulos and N. G. Bourbakis, “A Survey on Wearable Sensorbased systems for health monitoring and prognosis,” *IEEE T. Syst. Man. Cyb.*, vol. 40, no.1, pp. 1-12, Jan. 2010.

[10] T. Johnson, M. Valentinuzzi and L. Mertz, Are Wearable sensors safe?, *IEEE Pulse Magazine*, January 2016. Available at: https://pulse.embs.org/january-2016/are-wearables-safe/

[11] H. Z. Tan, L. Slivovsky, and A. Pentland, “A sensing chair using pressure distribution sensors,” *IEEE/ASME T. Mech.*, vol. 6, no. 3, pp. 261-268, Sept. 2001.

[12] T. Fu and A. Macleod, “IntelliChair: An Approach for Activity Detection and Prediction via Posture Analysis,” in *2014 Int. Conf. Intell. Env.* Shanghai, Jul. 2014, pp. 211-214.

[13] B. Arnrich, C. Setz, R. LaMarca, S. Troster and U. Ehlert, “What does your chair know about your stress level?,” *IEEE T. Inf. Technol. B.*, vol.14, pp. 207-214, Mar. 2010.

[14] E. Griffiths, T. S. Saponas and A. J. Brush, “Health Chair: Implicitly sensing heart and respiratory rate,” in *UBICOMP 2014*, Seattle, Washington, Sept. 2014, pp. 661-671.

[15] E. Pinheiro, O. Postolche and P. Girao, “Theory and developments in an unobtrusive cardiovascular system representation,” *Open Biomed. Eng. J.*, vol. 42, pp. 201-216, Oct. 2010.

[16] T. Klap and Z. Shinar, “Using piezoelectric sensor for continuouscontact-free monitoring of heart and respiration rates in real-life hospital settings,” in *Computing in Cardiology 2013*, Zaragoza, Sept. 2013, pp. 671-674.

[17] J. M. Kortelainen and J. Virkkala, “FFT averaging of multichannel BCG signals from bed mattress sensor to improve estimation of heart beat interval,” in *Proc. 29th Annu Int. IEEE Eng. Med. Biol. Soc. Conf.*, Lyon, Aug. 2007, pp. 6685-6688.

[18] M. Migliorini et al., “Automatic sleep staging based on ballistocardiographic signals recorded through bed sensors,” *Proc. 32nd Annu Int. IEEE Eng. Med. Biol. Soc. Conf.*, Buenos Aires, Nov. 2010, pp. 3273-3276.

[19] A. Akhbardeh, S. Junnila, M. Koivuluoma, T. K. Koivistoinen and A. Varri, “Evaluation of heart conditions based on ballistocardiogram classification using compactly supported wavelet transforms and neural networks,” in *Proc. of 2005 IEEE Conference on Control Applications*, Toronto, Ont., Aug. 2005, pp. 843-848.

[20] C. Bruser et al, “Automatic detection of atrial fibrillation in cardiac vibration signals,” *IEEE J. Biomed. Health. Inform.*, vol. 17, no.1, pp. 162-171, Jan. 2013.

[21] Xinsheng Yu, D. Dent and C. Osborn, “Classification of ballistocardiography using wavelet transform and neural networks,” in *Proc. 18th Annu Int. IEEE Eng. Med. Biol. Soc. Conf.*, Amsterdam, May 1996, pp. 937-938.

[22] S. Junnila, A. Akhbardeh, A. Varri and T. Koivistoinen, “An EMFifilm sensor based ballistocardiographic chair: performance and cycle extraction method,” in *IEEE Workshop on Signal Processing Systems Design and Implementation*, Athens, Greece, Nov. 2005, pp. 373-377.

[23] M. Enayati, B. Y. Su, M. Skubic, L. Despins, J. M. Keller and M. Popescu, “Investigating the interaction between ballistocardiogram and respiratory phases,” in *IEEE International Conference on Biomedical and Health Informatics*, Orlando, Florida, Feb. 2017.

[24] How a recliner is made. Available at: http://www.madehow.com/Volume3/Recliner.html

[25] B. Y. Su, K. C. Ho, M. Skubic, and L. Rosales, "Pulse rate estimation using hydraulic bed sensor," in *Proc. 34th Annu Int. IEEE Eng. Med. Biol. Soc. Conf.*, San Diego, California, Aug. 2012, pp. 2587-2590.

[26] O. T. Inan et al, "Ballistocardiography and Seismocardiography: A review of recent advances," *IEEE J. Biomed. Health*, vol. 19, no. 4, pp. 1414-1427, Jul. 2015.

[27] Tekscan pressure sensors and systems. Available at: https://www.tekscan.com/pressure-sensors

[28] TigerPlace is an assisted living center at Columbia, Missouri, USA. Available at: http://www.americareusa.net/location/tigerplace/

[29] S. Nurmi, Nocturnal Sleep quality and quantity analysis with Ballistocardiography, Aalto University. , 2016.

[30] P. A. Cain et al, "Age and gender specific normal values of left ventricular mass, volume and function for gradient echo magnetic resonance imaging: a cross sectional study," *BMC Med. Imaging*, vol. 9, Jan. 2009.

[31] R. Kumar, A. Bayliff, D. De, A. Evans, S. K. Das and M. Makos, "Care Chair: Sedentary activities and behavior assessment with smart sensing on chair backrest," in *2016 IEEE International Conference on Smart Computing*, St Louis, Missouri, May 2016, pp. 1-8.

[32] World Health Organization Fact sheets: Top 10 causes of death. Available at: http://www.who.int/mediacentre/factsheets/fs310/en/

[33] Centres for Disease Control and Prevention, "Depression is Not a Normal Part of Growing Older," Division of Population Health, updates January 31, 2017, Available at: https://www.cdc.gov/aging/mentalhealth/depression.htm.

[34] B. Sharma, R. Owens, A. Malhotra, "Sleep in Congestive Heart Failure," *Med Clin North Am.*, vol. 3, May 2010, pp. 447-464.

[35] K. L. Yang and T. J. Martin, "A Prospective Study of Indexes Predicting the Outcome of Trials of Weaning from Mechanical Ventilation," *New England Journal of Medicine*, vol. 324, no. 21, pp. 1445-1450, May 1991.

[36] K. Cluff et al, "Passive Wearable Skin Patch Sensor Measures Limb Hemodynamics Based on Electromagnetic Resonance," *IEEE Transactions on Biomedical Engineering*, vol. 65, no. 4, pp. 847-856, April 2018.

[37] L. C. DeSouza and J. R. Lugon, "The rapid shallow breathing index as a predictor of successful mechanical ventilation weaning: clinical utility when calculated from ventilator data," *J Bras Pneumol*, vol. 41, no. 6, pp. 530-535, Aug. 2015.

[38] S. H. GW and L. Park, "Variations in the measurement of weaning parameters: a survey of respiratory therapists," *Chest Journal*, vol. 121, no. 6, pp. 1947-1955, Jun. 2002.

[39] C. W. Seymour, B. J. Cross, C. R. Cooke, R. L. Gallop and B. D. Fuchs, "Physiologic Impact of Closed-System Endotracheal Suctioning in Spontaneously Breathing patients receiving mechanical ventilation ," *Respiratory Care,* vol. 54, no. 3, pp. 367-374, Mar. 2009.

[40] S. K. Epstein and R. L. Ciubotaru, "Influence of gender and endotracheal tube size on preextubation breathing pattern," *American Journal of Respiratory and Critical Care Medicine*, vol. 154, no. 6, pp. 1647-1652, Dec. 1996.

[41] B. P. Krieger, J. Isber, A. Breitenbucher, G. Throop and P. Ershowsky, “Serial Measurements of the Rapid-Shallow-Breathing Index as a predictor of Weaning Outcome in Elderly Medical patients,” *Chest Journal*, vol. 112, no. 4, pp. 1029-1034, Oct. 1997.

[42] M. A. Tanios, M. L. Nevins, K. P. Hendra, P. Cardinal, J. E. Allan, E. N. Naumova and S. K. Epstein, “A randomized, controlled trial of the role of weaning predictors in clinical decision making,” *Critical Care Medicine*, vol. 34, no. 10, pp. 2530-2535, Oct. 2006.

[43] A. K. Boutou et al, “Diagnostic accuracy of the rapid shallow breathing index to predict a successful spontaneous breathing trial outcome in mechanically ventilated patients with chronic obstructive pulmonary disease,” *IEEE Transactions on Biomedical Engineering*, vol. 65, no. 4, pp. 847-856, April 2018.

[44] W. Chatila, B. Jacob, D. Guaglionone and C. A. Manthous, “The unassisted respiratory rate-tidal volume ratio accurately predicts weaning outcomes,” *The American Journal of Medicine*, vol. 101, no. 1, pp. 61-67, Jul. 1996.

[45] J. Ruskin, R. J. Bache, J. C. Rembert, J. C. Greenfield, “Pressure-Flow Studies in Man: Effect of Respiration on left Ventricular Stroke Volume,” *Circulation Journal*, vol. 48, no. 1, pp. 79-85, Jul. 1973.

[46] J. Jalali, B. Y. Su, Breathing Index for analysing Sleep Apnea, University of Missouri-Columbia. , 2017.